Eur. Phys. J. C (2026) 86:590
https://doi.org/10.1140/epjc/s10052-026-15750-9

THE EUROPEAN PHYSICAL JOURNAL C

Regular Article - Theoretical Physics

Application of the 3-loop FlexibleEFTHiggs method to the MSSM and the NMSSM

Thomas Kwasnitza[1], **Dominik Stöckinger**[1], **Alexander Voigt**[2], **Johannes Wünsche**[1,a]

[1] Institut für Kern- und Teilchenphysik, TU Dresden, Zellescher Weg 19, 01069 Dresden, Germany
[2] Institute for Theoretical Solid State Physics, RWTH Aachen University, Sommerfeldstraße 16, 52074 Aachen, Germany

Received: 26 November 2025 / Accepted: 24 April 2026
© The Author(s) 2026

Abstract We perform an extensive analysis of the light CP-even Higgs boson pole mass in the MSSM and its dependencies on various parameters based on the 3-loop `FlexibleEFTHiggs` hybrid calculation which is implemented and publicly available since recently in `FlexibleSUSY`. Our focus lies on the study of the robustness of the approach in scenarios of highly non-degenerate SUSY mass spectra. Also, we present an improved Higgs mass calculation in the NMSSM based on the same approach, which is published in the new version 2.9.0 of `FlexibleSUSY` as well. The calculation provides a treatment in the full-model parametrization, leading to an advantageous resummation of QCD-enhanced terms in the stop-mixing parameter and includes important 2-loop contributions as well as 3-loop QCD contributions in the MSSM limit. We assess the reliability of this new calculation by applying it to several distinct NMSSM scenarios. In this context, special attention is devoted to the estimation of NMSSM-specific theory uncertainty.

Contents

1 Introduction
2 The FlexibleEFTHiggs method
3 Application to the MSSM
3.1 Model definition
3.2 Uncertainty estimation
3.2.1 High-scale uncertainty
3.2.2 Low-scale uncertainty
3.2.3 Combined uncertainty
3.3 Parameter dependencies
3.3.1 Dependence on M_3
3.3.2 Dependence on μ and m_A
3.3.3 Dependence on $(m_{\tilde{q}})_{33}$ and $(m_{\tilde{u}})_{33}$
3.4 Benchmark scenarios
4 Application to the NMSSM
4.1 Model definition
4.2 Matching details
4.3 Uncertainty estimation
4.4 Numerical results
4.4.1 Validation
4.4.2 NMSSM-specific effects
4.4.3 Benchmark scenarios for M_h^{exp}
5 Summary and outlook
A SUSY Les Houches input
References

1 Introduction

The discovery of a Higgs boson h by the ATLAS and CMS experiments [1,2] represents a milestone in our understanding of the physics of elementary particles, because it confirms the existence of the Higgs field generating the masses of elementary particles within the Standard Model of particle physics (SM). However, the SM cannot explain the mass M_h of the Higgs boson itself, because it is related to the quartic Higgs coupling $\hat{\lambda}_{\text{SM}}$, which is a free parameter of the SM. For this reason and because the SM cannot provide an explanation of phenomena such as dark matter or neutrino masses, models beyond the Standard Model (BSM) have been proposed. Among them is the class of supersymmetric models which are able to predict the order of magnitude of the Higgs boson mass M_h. However, these models also incorporate numerous new particles, which have not been directly observed yet. For this reason, if these new BSM particles exist, they either have masses M_S of the order of the electroweak scale or below, $M_S \lesssim M_Z$, but are difficult to produce, or their masses are beyond the currently accessible

[a] e-mail: johannes.wuensche@tu-dresden.de (corresponding author)

Published online: 01 June 2026

energy scale of high-energy physics experiments (beyond the electroweak scale), $M_S \gg M_Z$. For both scenarios, there exist well-developed methods to predict M_h with reasonable precision (see e.g. Ref. [3] for a review of available methods):

- In scenarios where $M_S \sim M_Z$, so-called fixed-order (FO) calculations, where quantum corrections up to a fixed loop order are taken into account, lead to a reasonable precision. However, the prediction of M_h with this method is imprecise if the loop contributions not taken into account are large, which is the case when $M_S \gg M_Z$.
- In scenarios where $M_S \gg M_Z$, so-called effective field theory (EFT) calculations, where large logarithmic higher-order contributions of $\mathcal{O}\left(\ln^n(M_Z^2/M_S^2)\right)$ are taken into account at all orders n, leading to a reasonable precision. However, the prediction of M_h within an effective field theory becomes imprecise if $M_S \lesssim M_Z$, because the method neglects contributions of $\mathcal{O}\left(v^2/M_S^2\right)$, where $v \approx 246\,\text{GeV}$ is the vacuum expectation value of the SM Higgs doublet.

Since the mass scale M_S of the new BSM particles is unknown, it is a-priori not clear which of the two methods (FO or EFT) to use for a specific BSM parameter point to obtain a precise prediction of M_h. Thus, a "hybrid" method combining the virtues of both the FO and EFT calculative approaches is very advantageous. There are currently two different hybrid FO/EFT methods realized in several implementations:

- The `FeynHiggs` hybrid method [4–9]: The first implementation of a hybrid calculation of the MSSM Higgs mass was part of the `FeynHiggs` version published in 2013. It combines the radiative corrections to the Higgs mass matrix obtained from the FO calculation with the numerically determined corrections from the EFT approach. Double-counting is circumvented by additionally subtracting contributions which are covered by both approaches.
- The `FlexibleEFTHiggs` method [10–12]: The hybrid method of `FlexibleEFTHiggs`, being proposed in 2016, follows another approach. Its essence consists in the usage of the Higgs pole mass matching in order to determine the quartic Higgs coupling $\hat{\lambda}_{\text{SM}}$ in the SM at M_S. It naturally allows the inclusion of terms suppressed by powers of v^2/M_S^2. Then, $\hat{\lambda}_{\text{SM}}$ is evolved down to the electroweak scale where the Higgs pole mass is calculated, analogously to the pure EFT approach. Similar hybrid Higgs mass calculations based on this approach are implemented in `SARAH/SPheno` [6] and `NMSSMCalc` [13].

The `FlexibleEFTHiggs` method was first introduced in Ref. [10] at the 1-loop level and was published in `FlexibleSUSY` 1.7.0 [14]. It was applied to the (real, flavour-conserving) MSSM, but also to the NMSSM, the MRSSM and the E_6SSM, and achieved a precision of NLO+LL. The 1-loop `FlexibleEFTHiggs` method was refined in `FlexibleSUSY` 2.0.0 [11], to avoid the inclusion of higher order large logarithmic contributions, resulting in a precision of NLO+NLL. In Ref. [12] the `FlexibleEFTHiggs` method was applied to the MSSM together with the inclusion of loop contributions from the literature up to (including) 2-loop and 3-loop level in the so-called "gaugeless limit" where the electroweak gauge couplings g and g' are set to zero. The achieved precision was thus of N^{3}LO+N^{3}LL in the strong coupling [15]. Furthermore, a full-model parametrization was used instead of an EFT-parametrization, leading to a very beneficial effective resummation of QCD-enhanced terms leading in the stop mixing parameter. The resulting calculation can be regarded as state-of-the-art, see Ref. [3]. For discussions of 2-loop corrections taking into account contributions involving the electroweak gauge couplings, see Ref. [16–19].

In the present paper, the application of `FlexibleEFTHiggs` to the MSSM at 3-loop level is further pursued by widening the focus from "standard" scenarios with degenerate SUSY mass spectra to generic scenarios where all mass parameters can be different. As one of our main purposes, we scrutinize the accuracy and reliability of the predictions also for such more general parameter choices in order to corroborate the robustness of the implemented calculation. This includes a check of the numerical stability of the implementation and the smallness of the theory uncertainty, where both rely on the correct cancellation of logarithmic terms in the matching relations. Also, various parameter dependences are revisited.

Our second focus lies on the NMSSM. In the context of Higgs mass calculation, this model has been analyzed extensively. However, only very few studies employed a hybrid calculative method for that purpose. The first hybrid calculation in the NMSSM was presented in Ref. [10] implementing the `FlexibleEFTHiggs` -method as a part of `FlexibleSUSY`. It included a 1-loop matching and achieved a precision of NLO+NLL after the refinement in `FlexibleSUSY` 2.0.0 [11], as mentioned above. Another hybrid calculation in the NMSSM based on the same algorighmic idea was presented in Ref. [13] and implemented in `NMSSMCalc` [13]. It realizes a 2-loop matching with MSSM-like 2-loop matching corrections of $\mathcal{O}\left(g_3^2 y_t^4 + y_t^6\right)$ as well as mixed strong-electroweak corrections from Ref. [17], however with terms suppressed by powers of v^2/M_S^2 only included up to 1-loop level.

As a second purpose of this publication, we present a newly implemented application of the `FlexibleEFTHiggs` method to the NMSSM with a 3-loop matching, i.e.

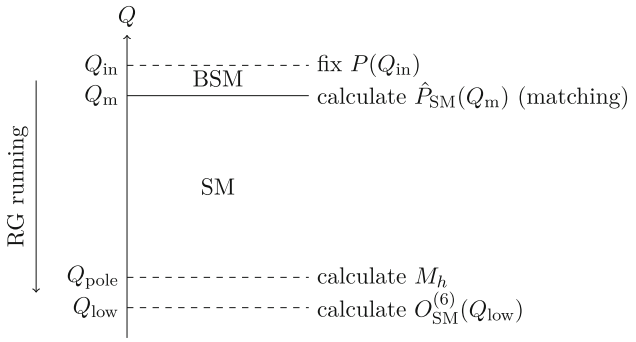

Fig. 1 Schematic illustration of the scales used in the refined `FlexibleEFTHiggs` method

including 2-loop matching corrections of $\mathcal{O}\left(g_3^2(y_t^4+y_b^4)\right)$ $\mathcal{O}\left(+(y_t^2+y_b^2)^3+(y_t^2+y_\tau^2)^3\right)$ and the dominant 3-loop corrections of $\mathcal{O}\left(y_t^4 g_3^4\right)$. The latter are provided by the module `Himalaya` [20,21] which uses different approximations from [22], selected according to the considered hierarchy between the gluino and the squark masses. This extension of the `FlexibleEFTHiggs` calculation in the NMSSM is publicly available since the recent version 2.9.0 of `FlexibleSUSY` and represents a code achieving state-of-the-art precision for the Higgs mass calculation in the NMSSM. Similar to the MSSM case, several scenarios and parameter dependences are analysed, and the theory uncertainty of the calculation is quantified by employing several methods of estimation.

2 The FlexibleEFTHiggs method

In this study we consider a calculation of the light CP-even Higgs pole mass M_h in the MSSM and the NMSSM. We employ a hybrid calculation that resums large logarithmic contributions of the form $\ln^n(M_Z^2/M_S^2)$ and at the same time includes complete series of terms of $\mathcal{O}\left(v^n/M_S^n\right)$. For our calculation we use the refined `FlexibleEFTHiggs` method described in detail in Ref. [12] and published in `FlexibleSUSY` 2.9.0.

The `FlexibleEFTHiggs` method is schematically illustrated in Fig. 1. It is structurally similar to a pure EFT calculation, where all BSM particles are integrated out at a common scale Q_m of the order of the BSM particle masses M_S, resulting in the SM as EFT. The obtained SM parameters are evolved down to the electroweak scale $Q_\mathrm{low} \approx M_Z$, using SM-renormalization group running, where they are matched to known low-energy observables. Due to this running large logarithmic contributions to M_h are effectively resummed when the Higgs pole mass is calculated in the SM at the electroweak scale. The special feature of the `FlexibleEFTHiggs` method lies in the matching conditions between the BSM model and the SM: To determine the quartic Higgs coupling $\hat{\lambda}_\mathrm{SM}(Q_\mathrm{m})$ in the SM, a Higgs pole mass matching condition of the form

$$(M_h^\mathrm{MSSM})^2 = (M_h^\mathrm{SM})^2 \tag{1}$$

is used. When the squared SM Higgs pole mass is written as

$$(M_h^\mathrm{SM})^2 = \hat{\lambda}_\mathrm{SM}(Q_\mathrm{m})\hat{v}^2 + \Delta s_h^\mathrm{SM}, \tag{2}$$

where Δs_h^SM are the SM loop corrections, one obtains the quartic Higgs coupling as

$$\hat{\lambda}_\mathrm{SM}(Q_\mathrm{m}) = \frac{1}{\hat{v}^2}\left[(M_h^\mathrm{MSSM})^2 - \Delta s_h^\mathrm{SM}\right]. \tag{3}$$

In the `FlexibleEFTHiggs` method the r.h.s. of Eq. (3) is expanded in loops and couplings, but not in powers of $\hat{v}/M_S$. In this way certain series of terms of the form $\mathcal{O}\left(v^n/M_S^n\right)$ are included in the value $\hat{\lambda}_\mathrm{SM}(Q_\mathrm{m})$. When the Higgs pole mass is eventually calculated at the electroweak scale in the SM using the value of $\hat{\lambda}_\mathrm{SM}(Q_\mathrm{pole} \approx M_t)$, both large logarithmic terms and terms of the form $\mathcal{O}\left(v^n/M_S^n\right)$ are included.

In the following we describe the `FlexibleEFTHiggs` method to calculate M_h in more detail. While Ref. [12] describes the method for the MSSM, we generalize it here to non-minimal supersymmetric models, such as the NMSSM. In the refined `FlexibleEFTHiggs` method the prediction of the Higgs pole mass M_h starts by specifying the parameters $P(Q_\mathrm{in})$ of the full (supersymmetric) BSM model in the $\overline{\mathrm{DR}}'$ scheme[1] at some user-chosen input renormalization scale Q_in, see Fig. 1. We divide these parameters into the following two subsets, $P(Q_\mathrm{in}) = P_\mathrm{SM}(Q_\mathrm{in}) \cup P_\mathrm{BSM}(Q_\mathrm{in})$:

- BSM parameters that have an SM counterpart. These are the three electroweak gauge couplings g_1, g_2 and g_3, the third generation Yukawa couplings y_t, y_b and y_τ and the SM-like vacuum expectation value v. We denote these parameters as

$$P_\mathrm{SM}(Q_\mathrm{in}) = \{g_1(Q_\mathrm{in}), g_2(Q_\mathrm{in}), g_3(Q_\mathrm{in}), y_t(Q_\mathrm{in}), y_b(Q_\mathrm{in}), y_\tau(Q_\mathrm{in}), v(Q_\mathrm{in})\}. \tag{4}$$

  These parameters are not free input parameters, because they will be fixed by measured low-energy quantities, see below.
- Pure BSM parameters $P_\mathrm{BSM}(Q_\mathrm{in})$, that have no SM counterpart. These are soft supersymmetry-breaking parameters, non-SM superpotential parameters (such as the μ parameter in the MSSM), non-SM vacuum expectation values (such as v_s in the NMSSM) and combinations thereof (such as $\tan\beta = v_u/v_d$ in the MSSM) etc. These

[1] The $\overline{\mathrm{DR}}'$ scheme differs from naive minimal substraction in the DR scheme by the renormalization of the unphysical ϵ-scalar mass. See [23] for details.

parameters are free input parameters and are not fixed by measurements.

All parameters $P(Q_{\rm in})$ of the BSM model are evolved to a the matching scale $Q_{\rm m}$ using the full 2-loop renormalization group equations from Refs. [23–35] with additional 3-loop MSSM contributions from Refs. [36,37], if appropriate. The matching scale $Q_{\rm m}$ should be chosen to be of the order of the non-SM BSM particle masses M_S, i.e. $Q_{\rm m} \sim M_S$.

At the single matching scale $Q_{\rm m}$, all BSM particles are integrated out leaving the SM as effective theory with a prediction of the SM $\overline{\rm MS}$ parameters

$$\hat{P}_{\rm SM}(Q_{\rm m}) = \Big\{\hat{g}_1(Q_{\rm m}), \hat{g}_2(Q_{\rm m}), \hat{g}_3(Q_{\rm m}), \hat{y}_t(Q_{\rm m}), \hat{y}_b(Q_{\rm m}), \hat{y}_\tau(Q_{\rm m}), \hat{v}(Q_{\rm m}), \hat{\lambda}_{\rm SM}(Q_{\rm m})\Big\} \tag{5}$$

from the BSM parameters $P(Q_{\rm m})$. The imposed matching conditions are described in detail in Ref. [12]. An important point w.r.t. this matching is the employed Higgs pole mass matching condition, which allows the inclusion of terms suppressed by powers of v^2/M_S^2 in the quartic SM Higgs coupling $\hat{\lambda}_{\rm SM}(Q_{\rm m})$ in a natural way. The matching conditions are solved perturbatively for the SM $\overline{\rm MS}$ parameters (5) at the matching scale in terms of loops, as described in Ref. [12]. For instance, for the SM quartic $\overline{\rm MS}$ Higgs coupling $\hat{\lambda}_{\rm SM}$ one obtains

$$\hat{\lambda}_{\rm SM}(Q_{\rm m}) = \frac{m_h^2(Q_{\rm m})}{v^2(Q_{\rm m})} + \Delta\lambda^{1\ell}_{\rm SM}(Q_{\rm m}) + \Delta\lambda^{2\ell}_{\rm SM}(Q_{\rm m}) + \Delta\lambda^{3\ell}_{\rm SM}(Q_{\rm m}), \tag{6}$$

where m_h is the SM-like $\overline{\rm DR}'$ Higgs mass in the BSM model and $\Delta\lambda^{k\ell}_{\rm SM}$ are the k-loop threshold corrections. In all BSM models the complete 1-loop threshold corrections are taken into account, including regularization conversion terms. In the MSSM and NMSSM we include threshold corrections of 2-loop order $\mathcal{O}\big(g_3^2(y_t^4+y_b^4) + (y_t^2+y_b^2)^3 + (y_t^2+y_\tau^2)^3\big)$ from Refs. [38–42] and of 3-loop order $\mathcal{O}\big(g_3^4 y_t^4\big)$ from Ref. [21]. There are two important features that distinguish Eq. (6) from pure effective field theory (EFT) calculations such as `SusyHD` [43] or `HSSUSY` [11,21]:

- The matching calculation, including e.g. the r.h.s. of Eqs. (3) or (6) is expressed as a perturbative expansion in terms of the BSM model parameters, i.e. not in terms of the SM parameters. In Ref. [12] this approach was therefore called "full-model parametrization". It has been shown in Ref. [15] that this full-model parametrization leads to an effective resummation of QCD-enhanced terms that involve (potentially large) trilinear squark–Higgs couplings in the MSSM. The same resummation effect is also present in the NMSSM. At the same time, the full-model parametrization substantially simplifies the application of the computational setup to non-minimal SUSY models such as the NMSSM or beyond.
- In the derivation of Eq. (6) no expansion in powers of v^2/M_S^2 is performed. Therefore $\hat{\lambda}_{\rm SM}(Q_{\rm m})$ contains terms of $\mathcal{O}\big(v^2/M_S^2\big)$ in an unexpanded form, which are not included in the pure-EFT calculations of `SusyHD` and `HSSUSY`. These terms are of importance in parameter scenarios that contain BSM particles with masses not large compared to the electroweak scale, i.e. where $v \sim M_S$. The inclusion of these terms leads to the specific feature that the Higgs boson pole mass calculated with the hybrid `FlexibleEFTHiggs` method converges to the fixed-order calculation for $M_S \to M_Z$ and to the pure-EFT calculation for $M_S \to \infty$ (as long as both calculations are expressed in terms of the same parameters).

The SM $\overline{\rm MS}$ parameters $\hat{P}_{\rm SM}(Q_{\rm m})$ from Eq. (5), which have been determined from the matching of the BSM model to the SM, are evolved to the electroweak scale $Q_{\rm low} = M_Z$ using the SM renormalization group equation with contributions up to the 4-loop level from Refs. [44–51]. The so-obtained SM $\overline{\rm MS}$ parameters $\hat{P}_{\rm SM}(Q_{\rm low})$ are then used to calculate the following SM quantities:

$$O^{(6)}_{\rm SM}(Q_{\rm low}) = \Big\{\alpha_{\rm em}^{\rm SM(6)}(Q_{\rm low}), \alpha_{\rm s}^{\rm SM(6)}(Q_{\rm low}), G_F, M_t, M_Z, m_b^{\rm SM(6)}(Q_{\rm low}), M_\tau\Big\}. \tag{7}$$

In Eq. (7) $\alpha_{\rm em}^{\rm SM(6)}(Q_{\rm low})$ and $\alpha_{\rm s}^{\rm SM(6)}(Q_{\rm low})$ denote the $\overline{\rm MS}$ electromagnetic and the strong couplings in the SM with six active quark flavours, respectively, G_F is the Fermi constant, M_t is the top quark pole mass, M_Z is the Z boson pole mass, $m_b^{\rm SM(6)}(Q_{\rm low})$ is the bottom quark $\overline{\rm MS}$ mass in the SM with six active quark flavours and M_τ is the τ lepton pole mass. The loop orders, at which these quantities are calculated, are chosen such that the desired precision of the prediction of M_h is reached, see Ref. [12] for details. The electromagnetic and strong couplings, as well as the $\overline{\rm MS}$ bottom quark mass from Eq. (7) are further converted to their $\overline{\rm MS}$ counterparts in the SM with only five active quark flavours. One thus arrives at the following set of low-energy quantities:

$$O^{(5)}_{\rm SM} = \Big\{\alpha_{\rm em}^{\rm SM(5)}(M_Z), \alpha_{\rm s}^{\rm SM(5)}(M_Z), G_F, M_t, M_Z, m_b^{\rm SM(5)}(m_b), M_\tau\Big\}. \tag{8}$$

The so-obtained low-energy quantities from Eq. (8) are compared to corresponding user-given low-energy input parameters. If the two parameter sets are not equal, the SM-like BSM parameters $P_{\rm SM}(Q_{\rm in})$ in Eq. (4) are varied until the two parameter sets match. This procedure is denoted as "shooting solver" in `FlexibleSUSY`.

Once a parameter set $P_{\rm SM}(Q_{\rm in})$ has been determined that is consistent with the user-given input the Higgs boson

pole mass M_h is calculated in the SM in the $\overline{\text{MS}}$ scheme at the renormalization scale $Q_{\text{pole}} = M_t$ using the parameters $\hat{P}_{\text{SM}}(Q_{\text{pole}})$. In this calculation we include the full 1-loop contributions, the 2-loop contributions of the order $\mathcal{O}\big(\hat{g}_3^2(\hat{y}_t^4\hat{v}^2 + \hat{y}_b^4) + (\hat{y}_t^2 + \hat{y}_b^2)^3\hat{v}^2 + (\hat{y}_t^2 + \hat{y}_\tau^2)^3\hat{v}^2\big)$ from Refs. [12,43,52,53] and the 3-loop contributions of $\mathcal{O}\big(\hat{g}_3^4\hat{y}_t^4\hat{v}^2\big)$ from Ref. [53]. The precision of this Higgs pole mass prediction is thus of N^{3}LO with a large-log resummation[2] of N^{3}LL in the product of couplings given above. In the MSSM this precision has been reached before in Refs. [12,54]. In the NMSSM, however, this precision has not been reached before, to the best of our knowledge.

3 Application to the MSSM

The refined `FlexibleEFTHiggs` method with the precision at N^{3}LO and N^{3}LL resummation as well as x_t-resummation has been described for the CP-conserving MSSM in detail in Ref. [12]. However, in this reference the application of the method to concrete scenarios was restricted to simplified "standard" scenarios with degenerate SUSY mass parameters. In this section, we extend the application to various non-trivial scenarios with non-degenerate SUSY mass parameters.

3.1 Model definition

We very briefly introduce some conventions used for the following discussion of the CP-conserving MSSM. The utilized conventions are those used in Ref. [12]. We define all MSSM parameters $P(Q) = P_{\text{SM}}(Q) \cup P_{\text{MSSM}}(Q)$ in the $\overline{\text{DR}}'$ scheme. The SM-like MSSM parameters $P_{\text{SM}}(Q)$ are denoted as in Eq. (4). By EWSB, the neutral components of the two MSSM Higgs doublets h_u and h_d acquire vacuum expectation values (VEVs), which we denote as v_u and v_d, defined as

$$\langle h_u \rangle = \frac{1}{\sqrt{2}}\begin{pmatrix} 0 \\ v_u \end{pmatrix} \quad \text{and} \quad \langle h_d \rangle = \frac{1}{\sqrt{2}}\begin{pmatrix} v_d \\ 0 \end{pmatrix}. \tag{9}$$

Accordingly, v_u and v_d represent the true minimum of the effective Higgs potential. Their ratio defines the tangent of the angle β via $\tan\beta = v_u/v_d$. Among the electrically neutral physical Higgs states is one CP-odd Higgs boson A and two CP-even Higgs bosons h and H with $m_h \leq m_H$. The $\overline{\text{DR}}'$ mass of the lighter state h is given by

$$m_h^2 = \frac{1}{2}\left[m_Z^2 + m_A^2 - \sqrt{\left(m_Z^2 + m_A^2\right)^2 - 4m_Z^2 m_A^2\cos^2(2\beta)}\right] \tag{10}$$

$$= m_Z^2\cos^2(2\beta) + \mathcal{O}\left(\frac{m_Z^4}{m_A^4}\right) \tag{11}$$

$$= \frac{1}{4}\left(g_Y^2 + g_2^2\right)v^2\cos^2(2\beta) + \mathcal{O}\left(\frac{v^4}{m_A^4}\right) \tag{12}$$

with $g_Y = \sqrt{5/3}\,g_1$ and $v^2 = v_u^2 + v_d^2 \approx (246\,\text{GeV})^2$. The loop contributions between m_h and the corresponding pole mass M_h are sensitive to the mixing among the third generation sfermions. This mixing is governed by the mixing parameters X_f, $f \in \{t, b, \tau\}$, which we define as

$$\begin{aligned} X_t &= A_t - \mu\cot\beta, \qquad X_b = A_b - \mu\tan\beta, \\ X_\tau &= A_\tau - \mu\tan\beta \end{aligned} \tag{13}$$

for the third generation sfermions $\tilde{f}_i, i \in \{1, 2\}$. Here, μ is the superpotential parameter describing the coupling between the Higgs doublet superfields $\hat{H}_u$ and $\hat{H}_d$. The A_f are the trilinear Higgs–sfermion–sfermion couplings. In addition, we define the dimensionless third generation sfermion mixing parameters

$$\begin{aligned} x_t &= \frac{X_t}{\left[(m_{\tilde{q}}^2)_{33}(m_{\tilde{u}}^2)_{33}\right]^{1/4}}, \quad x_b = \frac{X_b}{\left[(m_{\tilde{q}}^2)_{33}(m_{\tilde{d}}^2)_{33}\right]^{1/4}}, \\ x_\tau &= \frac{X_\tau}{\left[(m_{\tilde{l}}^2)_{33}(m_{\tilde{e}}^2)_{33}\right]^{1/4}}, \end{aligned} \tag{14}$$

where $m_{\tilde{q}}^2$, $m_{\tilde{u}}^2$ and $m_{\tilde{d}}^2$ are the soft-breaking squared mass parameter matrices of the left- and right-handed quark superpartners, respectively. Likewise, the soft-breaking squared mass parameter matrices for the left- and right-handed lepton superpartners are represented by $m_{\tilde{l}}^2$ and $m_{\tilde{e}}^2$, respectively. We denote the soft-breaking gaugino mass parameters as M_i, $i \in \{1, 2, 3\}$, where M_1 corresponds to the bino, M_2 corresponds to the wino and M_3 corresponds to the gluino mass. We use the symbol μ for MSSM's superpotential μ-parameter. Finally, we use the symbol M_S to denote a SUSY mass scale parameter, which describes the order of the non-SM BSM particle masses.

3.2 Uncertainty estimation

In order to assess the reliability of the Higgs pole mass prediction, we estimate its uncertainty in a similar manner as in Ref. [12]. Accordingly, we consider two contributions to the total uncertainty: a "high-scale uncertainty" to estimate missing contributions in the matching of the MSSM to the SM, and a

[2] Due to the single matching scale, at which all BSM particles are integrated out, the resummation affects only large logarithms $\ln(M_Z/M_S)$ while logarithms of BSM mass ratios are not resummed but only captured at the considered fixed loop order of the high-scale matching calculation.

"low-scale uncertainty" to estimate missing contributions in the calculation of the Higgs pole mass in the SM at the scale Q_{pole} and in the calculation of the low-scale quantities $O_{\text{SM}}^{(5)}$. Due the imposed pole mass matching conditions, series of power-suppressed terms of $\mathcal{O}\left(v^2/M_S^2\right)$ are included in the calculation by construction at the full 1-loop and Yukawa- and QCD-enhanced 2-loop level. We do not include a so-called "EFT uncertainty" that would correspond to missing power-suppressed terms (for example power-suppressed 2-loop electroweak terms or non-resummed power-suppressed large logarithms from the lack of running dimension-6 operators). The impact of such missing terms is expected to be significantly smaller than the high-scale uncertainty from e.g. non-power-suppressed missing electroweak corrections.

3.2.1 High-scale uncertainty

As in Ref. [12], we estimate the high-scale uncertainty by varying the matching scale $Q_{\text{m}} \in [Q_{\text{in}}/2, 2Q_{\text{in}}]$ while keeping Q_{in} unchanged. We take the resulting variation of M_h as uncertainty estimate,

$$\Delta M_h^{Q_{\text{m}}} = \max_{Q\in[Q_{\text{in}}/2,2Q_{\text{in}}]} \Big\{ \big| M_h(Q_{\text{m}} = Q_{\text{in}}) - M_h(Q_{\text{m}} = Q) \big| \Big\}. \tag{15}$$

This method is commonly used in the literature [13,43,55–58] and well-proven to be a reliable approach to estimate the missing MSSM-like higher order terms, at least for moderately large values of the stop mixing parameter ($|x_t| \leq 3$), see Ref. [12]. Here, we desist from additionally estimating the high-scale uncertainty by regarding implicit corrections at higher order and reparametrization terms, as this was necessary in Ref. [12] to cover missing terms of highest order in x_t. For $|x_t| \leq 3$, the high-scale uncertainty estimation via matching scale variation turned out to be sufficient. Since only moderate values of x_t are considered here and, furthermore, the study of the x_t-dependence is not the focus of this work, the procedure can accordingly be simplified.

3.2.2 Low-scale uncertainty

In accordance with Ref. [12], we employ two methods to estimate the low-scale uncertainty: The variation of the renormalization scale Q_{pole} for the calculation of the Higgs pole mass M_h in the SM and the variation of the loop order at which the top quark pole mass M_t is calculated in the SM from the $\overline{\text{MS}}$ parameters $\hat{P}_{\text{SM}}(Q_{\text{low}})$.

Pole mass scale variation. In analogy to the matching scale variation, we vary the pole mass scale Q_{pole}, at which the Higgs pole mass M_h is calculated in the SM, between $M_t/2$ and $2M_t$. We take the resulting variation of the Higgs pole mass as uncertainty estimate,

$$\Delta M_h^{Q_{\text{pole}}} = \max_{Q\in[M_t/2,2M_t]} \Big\{ \big| M_h(Q_{\text{pole}} = M_t) - M_h(Q_{\text{pole}} = Q) \big| \Big\}. \tag{16}$$

The so-defined uncertainty $\Delta M_h^{Q_{\text{pole}}}$ is an estimate of logarithmic renormalization scale dependent SM contributions, not included in our calculation of M_h.

Variation of top quark pole mass loop order. Another source of low-scale uncertainty is the truncation of the perturbation series for the calculation of the low-scale quantities $O_{\text{SM}}^{(5)}$. These low-scale quantities implicitly fix the SM parameters $\hat{P}_{\text{SM}}(Q_{\text{low}}) \setminus \{\hat{\lambda}_{\text{SM}}(Q_{\text{low}})\}$. The largest uncertainty can be attributed to the fixation of the SM $\overline{\text{MS}}$ top quark Yukawa coupling $\hat{y}_t$ from the top quark pole mass M_t. For the desired Higgs pole mass prediction at N^{3}LO with N^{3}LL resummation, 3-loop QCD corrections must be included in the relation between M_t and $\hat{y}_t$. We denote the Higgs mass, where up to 3-loop QCD contributions to M_t are included as $M_h^{y_t,3\ell}$. We then estimate the missing higher order contributions by including the available 4-loop QCD contribution from Ref. [59] in the calculation of M_t in the SM at the scale Q_{low}. The resulting Higgs pole mass is denoted as $M_h^{y_t,4\ell}$. We then take the variation of the predicted Higgs pole masses as uncertainty estimate

$$\Delta M_h^{y_t} = \left| M_h^{y_t,3\ell} - M_h^{y_t,4\ell} \right|, \tag{17}$$

which is in accordance with Ref. [12].

3.2.3 Combined uncertainty

In order to obtain an estimate of the high-scale uncertainty ΔM_h^{HS}, just one method was employed, namely the matching scale variation. For the low-scale uncertainty, two different approaches are applied. Since there is a significant overlap between the estimated missing higher-order terms in both methods, we proceed as in Ref. [12] and take the maximum of both estimates as combined low-scale uncertainty ΔM_h^{LS}. We eventually take the linear addition of the obtained high-scale and low-scale uncertainties as a conservative estimation for the total uncertainty ΔM_h:

$$\Delta M_h = \Delta M_h^{\text{LS}} + \Delta M_h^{\text{HS}} = \max\left\{ \Delta M_h^{Q_{\text{pole}}}, \Delta M_h^{y_t} \right\} + \Delta M_h^{Q_{\text{m}}}. \tag{18}$$

This approach is again in accordance with Ref. [12].

3.3 Parameter dependencies

In the past years, extensive scans have been performed to investigate the Higgs mass dependence on the numerous parameters of the MSSM. Mainly, the regarded scenarios

incorporated "standard" spectra with degenerate or nearly degenerate soft-breaking mass parameters, like the ones presented in Ref. [3]. Such standard scenarios have also been studied with the 3-loop `FlexibleEFTHiggs` calculation in Ref. [12]. In the following we extend the consideration by including scenarios with non-standard spectra. These scans also serve as a further practical test of the stability of the `FlexibleEFTHiggs` calulation.

If not stated otherwise, we set the following MSSM $\overline{\text{DR}}'$ parameters to a common SUSY mass scale M_S parameter in our analysis:

$$(m^2_{\tilde{f}})_{ij}(Q_{\text{in}}) = M_S^2\,\delta_{ij}, \quad f \in \{q, u, d, l, e\},\ i \in \{1, 2, 3\}, \tag{19a}$$

$$M_i(Q_{\text{in}}) = M_S, \quad i \in \{1, 2, 3\}, \tag{19b}$$

$$A_f(Q_{\text{in}}) = 0, \quad f \in \{u, d, c, s, b, e, \mu, \tau\}, \tag{19c}$$

$$\mu(Q_{\text{in}}) = m_A(Q_{\text{in}}) = M_S. \tag{19d}$$

We set the input scale Q_{in} equal to the matching scale Q_{m} and equal to the SUSY scale parameter M_S, i.e. $Q_{\text{in}} = Q_{\text{m}} = M_S$. In our study, we vary the stop mixing parameter $x_t(Q_{\text{in}})$ and fix $A_t(Q_{\text{in}})$ according to Eqs. (13)–(14). The low-scale parameters $O^{(5)}_{\text{SM}}$ are set to

$$\alpha_{\text{em}}^{\text{SM}(5)}(M_Z) = 1/127.916, \tag{20a}$$

$$\alpha_{\text{s}}^{\text{SM}(5)}(M_Z) = 0.1184, \tag{20b}$$

$$G_F = 1.1663787 \cdot 10^{-5}\,\text{GeV}^{-2}, \tag{20c}$$

$$M_t = 173.34\,\text{GeV}, \tag{20d}$$

$$M_Z = 91.1876\,\text{GeV}, \tag{20e}$$

$$m_b^{\text{SM}(5)}(m_b) = 4.18\,\text{GeV}, \tag{20f}$$

$$M_\tau = 1.777\,\text{GeV}. \tag{20g}$$

3.3.1 Dependence on M_3

First we study the impact of the Higgs pole mass M_h on the gluino mass parameter M_3. In Fig. 2 (left panel) we show M_h as a function of M_3 for the fixed values $M_S = 3\,\text{TeV}$, $\tan\beta = 12$ and $x_t = 2$ (red solid line with red uncertainty band). The brown band marks the experimental value $M_h = (125.20 \pm 0.11)\,\text{GeV}$ [60]. In the range $M_3 \in [10^2, 5 \cdot 10^3]\,\text{GeV}$ the Higgs mass M_h is nearly independent of M_3, up to deviations of less than 1 GeV. At the same time, the estimated uncertainty ΔM_h remains essentially constant and of the order of $\Delta M_h \approx 1\,\text{GeV}$, underlining the robustness of the used `FlexibleEFTHiggs` method in this range. However, for M_3 notably larger than M_S, the calculated Higgs pole mass and especially its uncertainty increase significantly. The rise in the Higgs mass is a consequence of 2-loop corrections to $\hat{\lambda}_{\text{SM}}(Q_{\text{m}})$ of $\mathcal{O}\left(g_3^2 y_t^4\right)$, which contain terms quadratic in M_3 that stem from gluino-induced stop self-energy corrections. A detailed analysis of the terms can be found in Ref. [38].

The observed increased size of the uncertainty for large values of M_3 can be ascribed to the high-scale uncertainty determined via matching scale variation. As explained in Ref. [57], the gluino mass parameter appears linearly in the 1-loop renormalization group equation of x_t and quadratically in those of the squark mass parameters. Larger M_3 therefore imply an enhancement of the respective MSSM parameters during renormalization group running. As a consequence, changes in Q_{m} have a stronger impact on the numerical values of these parameters. Due to the strong sensitivity of the Higgs pole mass to x_t and to the squark mass parameters, M_h undergoes large variations while varying Q_{m}, which results in a large theory uncertainty. The large differences between the stop pole masses and their corresponding squark mass parameters, $(m_{\tilde{q}})_{33}$ and $(m_{\tilde{u}})_{33}$, visible for $M_3 \gg M_S$ in Fig. 2 (left panel) indicate that a more physical renormalization scheme may be very beneficial to stabilize the calculation. In Ref. [22], the so-called $\overline{\text{MDR}}$ renormalization scheme was suggested as an appropriate scheme to alleviate the problem. In Ref. [58], this scheme was applied to an EFT calculation of M_h leading to a substantial reduction of the estimated uncertainty. Currently, a treatment of that kind is not implemented in `FlexibleSUSY`.

In Fig. 2 (right panel), we show the dependence of M_h as a function of x_t for different values of the gluino mass parameter and fixed $M_S = 3\,\text{TeV}$ and $\tan\beta = 12$. It shows that changes in M_3 lead to a clear deformation of the curve of M_h as a function of x_t, including a change in the extent of the asymmetry and a compression in x_t-direction. Conversely, this implies a notable M_3-dependence of the values of x_t required to reproduce the experimental M_h. This interplay between M_3, x_t and M_h can be traced back to the 2-loop QCD contributions to M_h^2, which are linear in M_3 and odd in x_t, thus being responsible for a stronger asymmetry with growing M_3, c.f. Refs. [38,55]. Also, the strong x_t-dependence of the uncertainty for $M_3 = 9\,\text{TeV}$ is remarkable, especially the strong increase for $|x_t| > 1.5$. This again demonstrates that the effect of huge uncertainties for large M_3 is closely connected to the value of x_t.

3.3.2 Dependence on μ and m_A

In Fig. 3, we show the dependence of M_h on the $\overline{\text{DR}}'$ CP-odd MSSM Higgs mass m_A (left panel) and on the μ-parameter (right panel) for $M_S = 3\,\text{TeV}$, $\tan\beta = 20$ and $x_t = -2.2$. We find that a variation of m_A, even by orders of magnitude, has no large impact on M_h for the chosen value of $\tan\beta$. For smaller values of $\tan\beta$, a more relevant dependence can occur, this would however also require significantly larger M_S in order to obtain sufficiently large corrections to M_h. In contrast, a variation of μ between $-5\,\text{TeV}$

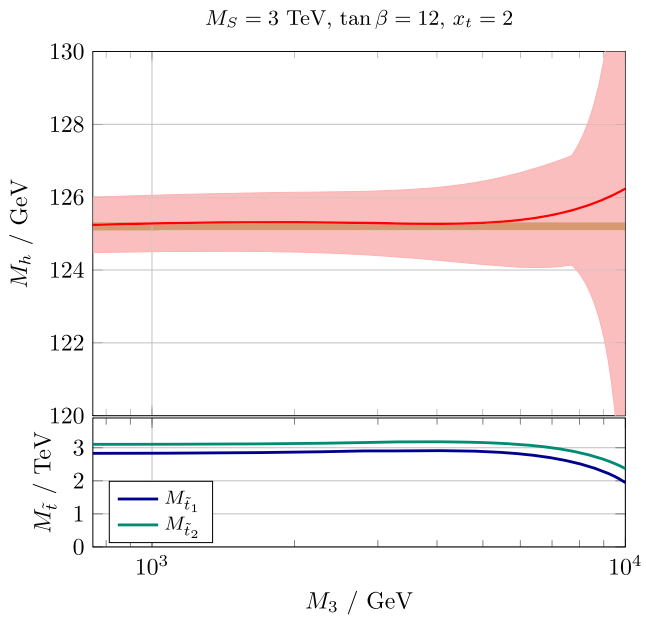

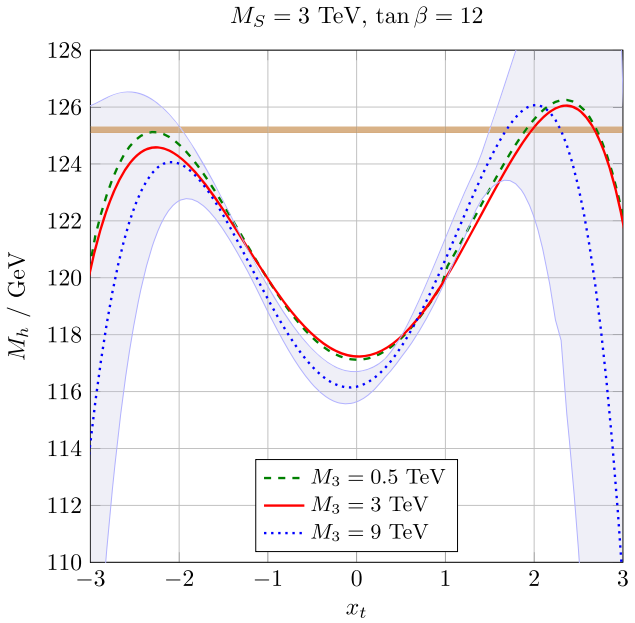

Fig. 2 Left panel: Dependence of M_h (and the stop pole masses $M_{\tilde{t}_{1,2}}$) on the gluino mass parameter M_3 with all other parameters fixed as in Eq. (19). The kink in the red uncertainty band at $M_3 \approx 8$ TeV originates from the high-scale uncertainty determined according to Eq. (15). At that point, the maximal difference is no longer found at the upper end of the $Q_{\rm m}$ variation interval but at the lower one. Right panel: Dependence of M_h on the stop mixing parameter x_t for different values of M_3. For $M_3 = 9$ TeV, the uncertainty is drawn as light blue band

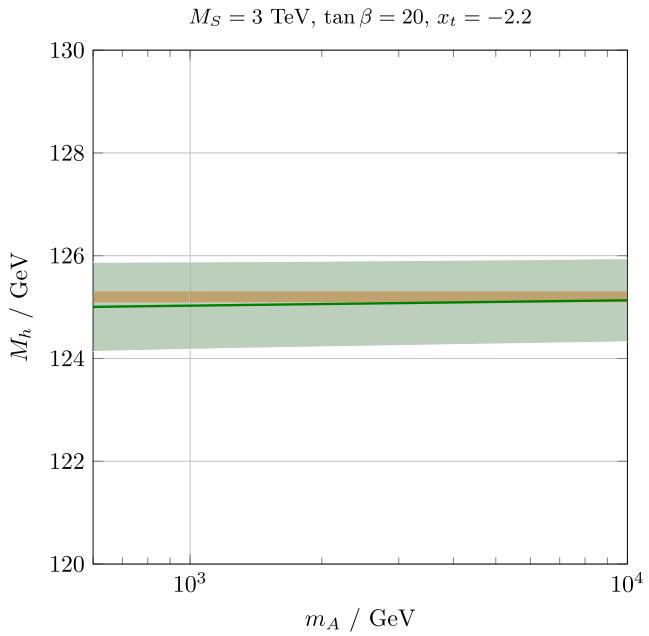

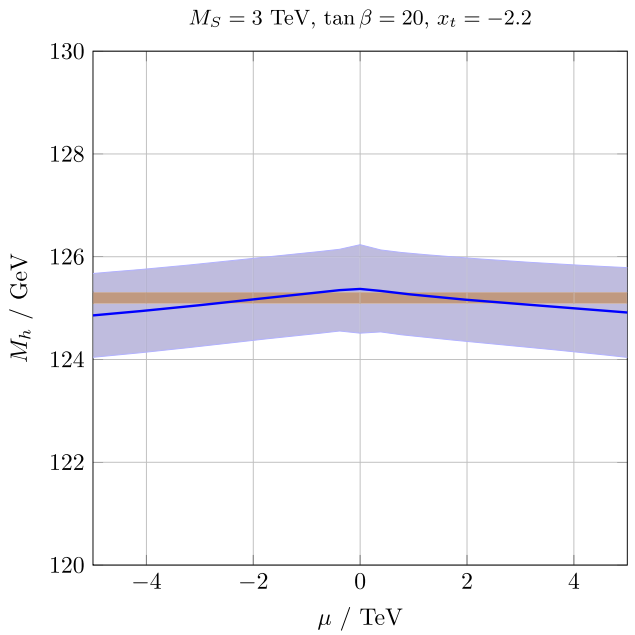

Fig. 3 Left panel: M_h as a function of the $\overline{\rm DR}'$ CP-odd Higgs mass m_A. Right panel: M_h as a function of the μ-parameter. The parameters not varied are fixed to $M_S = 3$ TeV, $\tan\beta = 20$ and $x_t = -2.2$. The green band (left panel) and the blue band (right panel) show the uncertainty ΔM_h. The brown band corresponds to the measured Higgs mass with its experimental uncertainty

and 5 TeV leads to a mild change in M_h of about 1 GeV, where larger $|\mu|$ imply smaller M_h. These results are fully in accordance with numerous analyses performed in the past [61–64]. For both dependencies, the corresponding uncertainty remains nearly constant with a numerical value of about 0.8 GeV. Merely for large μ, a slightly increased uncertainty can be noticed.

We note that the shown parameter regions in Fig. 3 contain points with very split SUSY mass spectra. At the same time we find that the predictions of M_h with the `FlexibleEFTHiggs` method is numerically stable in these regions. Nontheless, in regions with large, positive x_t and $m_A \ll M_S$, negative m_A^2 may occur during the renormalization group running and the `FlexibleEFTHiggs` calculation breaks down. This issue has been discussed in Ref. [54] in the context of a fixed-order $\overline{\text{DR}}'$ calculation. To study such regions with tachyonic m_A an effective field theory with a light m_A could be beneficial.

3.3.3 Dependence on $(m_{\tilde{q}})_{33}$ and $(m_{\tilde{u}})_{33}$

In Fig. 4 we show the dependence of M_h on the sfermion mass parameters $(m_{\tilde{q}})_{33}$ (left panel) and $(m_{\tilde{u}})_{33}$ (right panel) for different values of x_t. Here, the strong impact of the induced change in the $\overline{\text{DR}}'$ stop masses $m_{\tilde{t}_{1,2}}$ on the Higgs mass M_h becomes evident, which is much more significant than a change of M_3, m_A or μ. This high sensitivity originates from stop-induced 1-loop corrections to M_h. The two plots reveal a strong similarity in the dependence of M_h on the two sfermion mass parameters. Especially, the corresponding curves for the same fixed value of x_t have a very similar shape. Furthermore we find that M_h can be maximized if $(m_{\tilde{q}})_{33}$ and $(m_{\tilde{u}})_{33}$ are chosen appropriately, again for a given value of x_t.

It is important to note that the results given in the plots of Fig. 4 represent the outcome of the `FlexibleEFTHiggs` calculations with a matching at 2-loop level, except for the black dashed lines, which were obtained from a 3-loop matching for $x_t = 2$. The shown uncertainty band is depicted for the 2-loop calculations for $x_t = 2$. The uncertainty is found to remain nearly constant within the shown parameter range with numerical values slightly below 1 GeV. While the 2-loop curves and their uncertainties attest a good stability of the `FlexibleEFTHiggs` calculation, the 3-loop results are subject to several noteworthy jumps. This behaviour can be traced back to the 3-loop threshold corrections for $\hat{\lambda}_{\text{SM}}$ provided by `Himalaya` [20,21], for which different approximations are applied depending on the present hierarchy between gluino and squark masses. Hierarchy transitions taking place during the variation of an individual squark mass parameter then induce discontinuities in the numerical value of M_h. Also, it must be emphasized that for $(m_{\tilde{q}})_{33} \gtrsim 4\,\text{TeV}$ there is no suitable hierarchy implemented, leading to an absence of all 3-loop contributions in the matching of the BSM to the SM. This statement analogously holds for $(m_{\tilde{u}})_{33}$. However, the discontinuity at that threshold is hardly visible in the plots.

This analysis indicates that the 3-loop calculation is stable and precise in case of scenarios with degenerate mass spectra, especially for $(m_{\tilde{q}})_{33} \sim M_S$ and $(m_{\tilde{u}})_{33} \sim M_S$. However, it also reveals that in scenarios with non-degenerate squark masses the calculation becomes unstable due to the mentioned hierarchy transitions. In such cases, the 2-loop result can be regarded as more trustworthy.

3.4 Benchmark scenarios

Finally, we want to identify phenomenologically interesting regions of the MSSM parameter space which do not correspond to "standard" scenarios with degenerate mass parameters. For that porpose, a random scan is performed for which the MSSM parameters $P_{\text{BSM}}(Q_{\text{in}})$ are varied in the following ranges:

$$M_S = (m_{\tilde{f}})_{11} = (m_{\tilde{f}})_{22} = 3\,\text{TeV}, \qquad 1 \leq \tan\beta \leq 20, \tag{21a}$$

$$1\,\text{TeV} \leq (m_{\tilde{f}})_{33} \leq 5\,\text{TeV}, \qquad 1\,\text{TeV} \leq M_1, M_2, M_3 \leq 5\,\text{TeV}, \tag{21b}$$

$$1\,\text{TeV} \leq \mu \leq 5\,\text{TeV}, \qquad 1\,\text{TeV} \leq m_A \leq 5\,\text{TeV}, \tag{21c}$$

$$-10.5\,\text{TeV} \leq X_t \leq 10.5\,\text{TeV}, \quad -135\,\text{TeV} \leq X_b \leq 135\,\text{TeV}, \tag{21d}$$

$$A_f = 0, \tag{21e}$$

where $\tilde{f} \in \{\tilde{q}, \tilde{u}, \tilde{d}, \tilde{l}, \tilde{e}\}$ and $f \in \{u, d, c, s, e, \mu, \tau\}$. The soft-breaking trilinear Higgs coupling parameters A_t and A_b are chosen according to the values of X_t and X_b using Eqs. (13). Below, we will indicate the squark mixing in each scenario with the dimensionless mixing parameters x_t and x_b.

From all the generated parameter points, we first extracted all those which ensure vacuum stability and reproduce approximately the experimental value of the light SM-like Higgs boson mass $M_h \approx 125\,\text{GeV}$. It is well-known that $\tan\beta$ and the three stop-sector parameters ($(m_{\tilde{q}})_{33}$, $(m_{\tilde{u}})_{33}$ and x_t) strongly affect the Higgs mass M_h. Large $\tan\beta$, $(m_{\tilde{q}})_{33}$ and $(m_{\tilde{u}})_{33}$ as well as $|x_t| \approx \sqrt{6}$ tend to increase M_h significantly, such that this pattern is also common among the parameter points reproducing the experimental value. In detail, however, the required values of $\tan\beta$ and the three stop-sector parameters depend on the non-degeneracy within the stop sector and on all remaining parameters.

One finding worth mentioning is that all experimentally viable parameter scenarios were found to have $\tan\beta \gtrsim 6$, given $1\,\text{TeV} \leq (m_{\tilde{f}})_{33} \leq 5\,\text{TeV}$. Furthermore, from our scans we found that in all these scenarios the stop mixing parameter x_t lies in the range $1.3 \lesssim |x_t| \lesssim 3.2$. One should note that this behaviour with respect to the parameters $\tan\beta$ and x_t depends significantly on the chosen variation range of $(m_{\tilde{f}})_{33}$.

The resulting viable parameter points emerging from the scan can be divided into groups with similar characteristics.

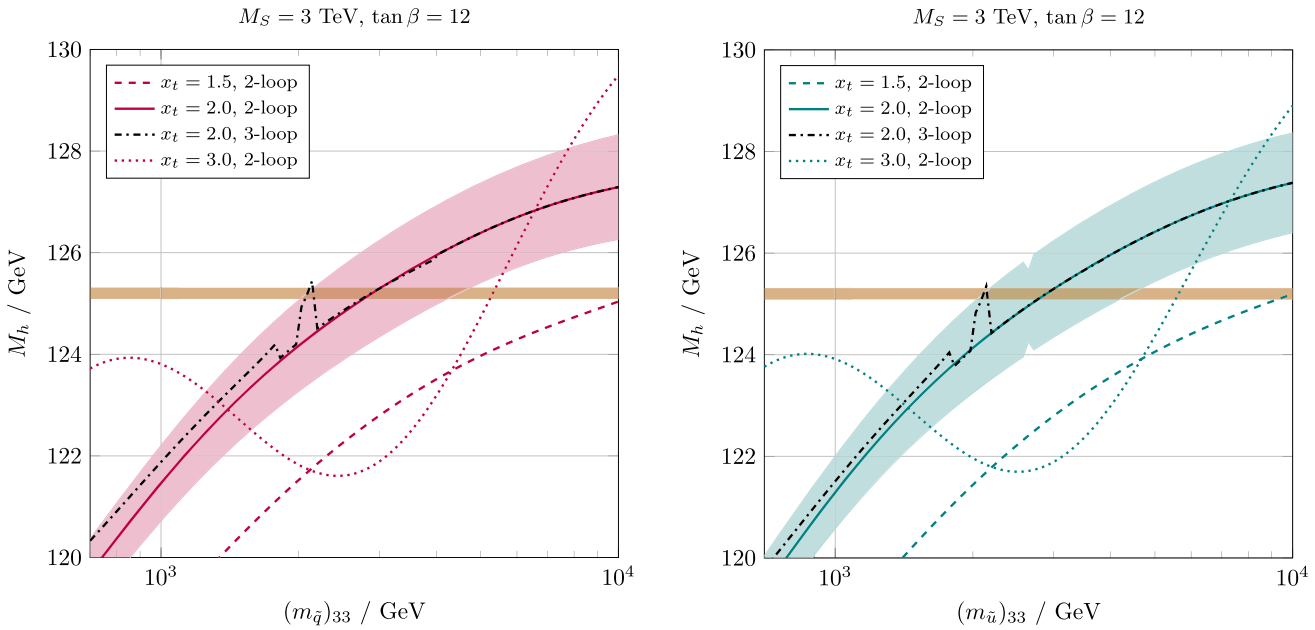

Fig. 4 Left panel: M_h as a function of $(m_{\tilde{q}})_{33}$ for different values of x_t. Right panel: M_h as a function of $(m_{\tilde{u}})_{33}$ for different values of x_t. The parameters not varied are fixed to $M_S = 3$ TeV and $\tan\beta = 12$. All curves are obtained from a 2-loop matching except the black dashed ones which represent the 3-loop results only for $x_t = 2$. Also for $x_t = 2$, the uncertainty bands (corresponding to the 2-loop calculation) are drawn in red (left panel) and teal (right panel), respectively. The brown band corresponds to the measured Higgs mass with its experimental uncertainty

Table 1 Selected MSSM benchmark points inspired by the result of the parameter scan specified in Eq. (21)

BMP	M0	M1	M2	M3	M4	M5
$\tan\beta$	12	6	20	20	8	9
M_1/GeV	3000	3000	3000	3000	3000	5000
M_2/GeV	3000	1200	1500	3000	3000	4200
M_3/GeV	3000	3000	4000	3000	3000	3000
m_A/GeV	3000	3000	3000	3000	3000	4800
μ/GeV	3000	1500	1200	3000	3000	3000
$(m_{\tilde{q}})_{33}$/GeV	3000	4500	4500	1000	3800	1500
$(m_{\tilde{u}})_{33}$/GeV	3000	3000	4500	5000	1000	1500
$(m_{\tilde{d}})_{33}$/GeV	3000	3000	2000	3000	3000	4500
$(m_{\tilde{l}})_{33}$/GeV	3000	3000	3000	3000	3000	3000
$(m_{\tilde{e}})_{33}$/GeV	3000	3000	3000	3000	3000	4500
x_t	2.2	2.25	−1.4	−3.0	3.1	−1.25
x_b	−16.5	−15.0	−32.5	0.0	5.0	38.0

In order to study the properties of interesting scenarios with the `FlexibleEFTHiggs` calculation, we chose one representative benchmark point from each group. The selected benchmark points are listed below, including a brief description of their characteristics:

- **(M0)** represents a standard scenario with degenerate SUSY mass spectrum and serves as a reference for the other benchmark points with non-degenerate mass spectra. Parameter points of that kind have been thoroughly analyzed in Ref. [12].
- **(M1)** is characterized by a small value of $\tan\beta$. During the scan, no parameter points with smaller values of $\tan\beta$ have been found that reproduce the experimental value of the Higgs mass.
- **(M2)** was chosen due to the fact that its value of $|x_t|$ differs strongly from $\sqrt{6}$.

Table 2 Higgs pole mass spectra for the MSSM benchmark points from Table 1. The estimated total uncertainty ΔM_h for the SM-like Higgs boson pole mass is also listed

BMP	M0	M1	M2	M3	M4	M5
M_h/GeV	125.29	125.37	125.09	124.96	125.03	125.02
ΔM_h/GeV	0.84	0.87	0.65	0.29	1.64	4.32
M_H/GeV	3041.17	3069.30	2115.23	1425.90	2919.65	4395.62
M_A/GeV	3041.22	3069.16	2115.50	1425.96	2919.76	4395.04
$M_{H^\pm}$/GeV	3041.85	3067.68	886.72	1225.21	2917.66	3339.8

- **(M3)** has the feature that $(m_{\tilde{q}})_{33}$ is significantly smaller than $(m_{\tilde{u}})_{33}$ and all other soft SUSY-breaking mass parameters.
- **(M4)** is characterized by a value of $(m_{\tilde{u}})_{33}$ being significantly smaller than $(m_{\tilde{q}})_{33}$ and all other soft SUSY-breaking mass parameters.
- **(M5)** features a small value of $(m_{\tilde{q}})_{33}$ and $(m_{\tilde{u}})_{33}$ at the same time.

The explicit numerical values of the parameters at the benchmark points can be found in Table 1. The Higgs mass spectra for these scenarios, obtained with the `FlexibleEFTHiggs` method at 3-loop level, are given in Table 2. First of all, one should take note of the result for (M0), which exemplifies again the findings of the study performed in Ref. [12], where for standard scenarios with degenerate SUSY mass spectra and $x_t \lesssim 3$ theoretical uncertainties of roughly that order were ascertained. Comparing it to the other benchmark points indicates that at least for a considerable fraction of the scenarios from distinct regions one finds uncertainties of about the same size. However, for other scenarios, especially (M5), one determines a significantly higher uncertainty of more than 4 GeV. In this particular case, the large uncertainty can be attributed to two sources. One origin are the abovementioned instabilities in the calculation of the 3-loop matching corrections $\mathcal{O}(g_3^4 y_t^4)$ from the `Himalaya` library, connected to transitions between different implemented mass hierarchies during matching scale variation. The second origin is the huge value of x_b, which provokes drastic changes in the numerical values of $(m_{\tilde{q}})_{33}$ and $(m_{\tilde{d}})_{33}$ during renormalization group running. Together they lead to a large variation of the calculated M_h for varying Q_m. With regard to these findings, it appears questionable whether the experimental Higgs mass can be reasonably predicted at the benchmark point (M5) with its remarkably small value of $|x_t|$.

As mentioned above, it is well-known that in particular large $\tan\beta$ and $|x_t| \sim \sqrt{6}$ yield large values of M_h. Some of the benchmark points (M1)–(M5) do not fulfill these two conditions. Accordingly, other mecanisms are present that compensate the negative effect on the size of the Higgs mass. One aspect contributing positively are clearly large values of the squark mass parameters, which increase the stop masses and thus induce an enhancement of M_h. This effect is very obvious in (M2), where $|x_t|$ differs strongly from $\sqrt{6}$, but very large $(m_{\tilde{q}})_{33}$ and $(m_{\tilde{u}})_{33}$ lead to a compensation of that negative effect. Also, a very small value of either of the two squark mass parameters can be compensated by a large value of the other one, respectively. This interplay occurs e.g. in (M3) and (M4).

4 Application to the NMSSM

4.1 Model definition

The NMSSM extends the field content of the MSSM by a gauge singlet chiral superfield $\hat{S}$. In the following we consider the Z_3-invariant NMSSM with the superpotential

$$W = Y_d \left(\hat{H}_d \cdot \hat{Q}\right) \hat{D} - Y_u \left(\hat{H}_u \cdot \hat{Q}\right) \hat{U} + Y_e \left(\hat{H}_d \cdot \hat{L}\right) \hat{E} - \lambda \hat{S} \left(\hat{H}_d \cdot \hat{H}_u\right) + \frac{\kappa}{3} \hat{S}^3, \tag{22}$$

where $\hat{A} \cdot \hat{B} := \epsilon_{DE} \hat{A}^D \hat{B}^E$ is the $SU(2)$-invariant product of the two superfields $\hat{A}$ and $\hat{B}$. Generation and colour indices are omitted here again for the sake of clarity. The NMSSM-specific couplings λ and κ are assumed to be real in order to avoid CP-violation in the Higgs sector. The superpotential term governed by the coupling λ replaces the analogous μ-term in the MSSM. In this way, the NMSSM provides a solution to the so-called μ-problem of the MSSM [65,66] by dynamically generating an effective μ-parameter if the scalar component s of the superfield $\hat{S}$ acquires a vacuum expectation value:

$$\mu_\mathrm{eff} = \frac{\lambda v_s}{\sqrt{2}} \quad \text{with} \quad \frac{v_s}{\sqrt{2}} = \langle s \rangle. \tag{23}$$

The soft-breaking Lagrangian of the NMSSM is given by

$$\mathcal{L}_\mathrm{soft} = -\tilde{q}^\dagger m_{\tilde{q}}^2 \tilde{q} - \tilde{u}_R^\dagger m_{\tilde{u}}^2 \tilde{u}_R - \tilde{d}_R^\dagger m_{\tilde{d}}^2 \tilde{d}_R - \tilde{l}^\dagger m_{\tilde{l}}^2 \tilde{l} - \tilde{e}_R^\dagger m_{\tilde{e}}^2 \tilde{e}_R - m_{h_d}^2 h_d^\dagger h_d - m_{h_u}^2 h_u^\dagger h_u - m_s^2 |s|^2 - \frac{1}{2}\left(M_1 \tilde{B}\tilde{B} + M_2 \tilde{W}_a \tilde{W}_a + M_3 \tilde{g}\tilde{g} + \text{h.c.}\right)$$

$$- \Big[(h_d \cdot \tilde{q}_L) T_d \tilde{d}_R^* - (h_u \cdot \tilde{q}_L) T_u \tilde{u}_R^* + (h_u \cdot \tilde{l}_L) T_e \tilde{e}_R^* - \lambda A_\lambda s\, (h_d \cdot h_u) + \frac{\kappa}{3} A_\kappa s^3 + \text{h.c.}\Big], \tag{24}$$

where $(T_f)_{ij} = (A_f)_{ij}(Y_f)_{ij}$. For the couplings λ and κ, a perturbativity limit can be formulated at the SUSY scale by demanding the absence of a Landau pole below the GUT scale. Using the corresponding β-functions from Ref. [67],

$$\beta_\lambda = \frac{\mathrm{d}\lambda}{\mathrm{d}(\ln Q)} = \kappa_L \left(4\lambda^3 + 2\lambda\kappa^2 + 3\lambda y_t^2 - \frac{3}{5}\lambda g_1^2 - 3\lambda g_2^2\right) + \mathcal{O}\left(\kappa_L^2\right), \tag{25}$$

$$\beta_\kappa = \frac{\mathrm{d}\kappa}{\mathrm{d}(\ln Q)} = \kappa_L \left(6\lambda^2\kappa + 6\kappa^3\right) + \mathcal{O}\left(\kappa_L^2\right), \tag{26}$$

where $\kappa_L = 1/(4\pi)^2$, that limit can be found to be approximately [68]:

$$\sqrt{\lambda^2 + \kappa^2} < 0.7. \tag{27}$$

The Higgs potential resulting from the NMSSM Lagrangian is given by

$$\begin{aligned} V_H = {} & \frac{g_1^2 + g_2^2}{8}\left(h_d^\dagger h_d - h_u^\dagger h_u\right)^2 + \frac{g_2^2}{2}\left|h_d^\dagger h_u\right|^2 \\ & + \lambda^2 |s|^2 \left(h_u^\dagger h_u + h_d^\dagger h_d\right) + \left|\lambda (h_u \cdot h_d) + \kappa s^2\right|^2 \\ & + m_{h_d}^2 h_d^\dagger h_d + m_{h_u}^2 h_u^\dagger h_u + m_s^2 |s|^2 \\ & + \left[\lambda A_\lambda s (h_u \cdot h_d) + \frac{\kappa}{3} A_\kappa s^3 + \text{h.c.}\right]. \end{aligned} \tag{28}$$

The potential is required to be configured such that all Higgs fields acquire a vacuum expectation value (VEV) by electroweak symmetry breaking. The VEVs of the Higgs doublets h_u and h_d are denoted as v_u and v_d, respectively, and are defined as in the MSSM, c.f. Eq. (9). In this work, we restrict ourselfs to the CP-conserving NMSSM. In order to circumvent CP violation in the Higgs sector, all VEVs are assumed to be real. Furthermore, all parameters appearing in the Higgs sector are accordingly chosen to be real and the CKM matrix is set to unity. As CP is conserved, CP-even and CP-odd neutral Higgs fields do not mix. There is however a mixing within the CP-even and the CP-odd Higgs sectors, respectively:

$$\begin{aligned} &\Re(h_u^0), \Re(h_d^0), \Re(s) \;\longrightarrow\; h_1, h_2, h_3, \\ &\Im(h_u^0), \Im(h_d^0), \Im(s) \;\longrightarrow\; A_1, A_2, G^0 \end{aligned} \tag{29}$$

with the CP-even mass eigenstates h_1, h_2 and h_3, the CP-odd ones A_1 and A_2 as well as the Goldstone boson G^0. Diagonalizing the CP-even Higgs boson mass matrix, the tree-level mass of lightest mass eigenstate h_1, which is assumed to correspond to the SM-like Higgs boson h, is found to be:

$$m_h^2 = m_Z^2 \cos^2(2\beta) + \lambda^2 v^2 \sin^2(2\beta) - \frac{\left[\sqrt{2}\lambda^2 v_s - \lambda(A_\lambda + \sqrt{2}\kappa v_s)\sin(2\beta)\right]^2 v^2}{\kappa v_s(\sqrt{2}A_\kappa + 4\kappa v_s)}, \tag{30}$$

in the limit of $v \ll m_A$ and $v \ll \kappa v_s(\sqrt{2}A_\kappa + 4\kappa v_s)$ (where the right side of the second inequality corresponds to the tree-level mass of the singlet scalar), i.e. keeping only leading terms of $\mathcal{O}(v^2)$ (see also Ref. [69]). The first term originates from the D-terms, the second one from F-terms and the third one from the decoupling to the singlet scalar component. Thus the NMSSM contains the following set of non-SM $\overline{\text{DR}}'$ input parameters:

$$\begin{aligned} P_{\text{NMSSM}}(Q_{\text{in}}) = {} & [P_{\text{MSSM}}(Q_{\text{in}}) \setminus \{\mu(Q_{\text{in}}), B\mu(Q_{\text{in}})\}] \\ & \cup \Big\{\lambda(Q_{\text{in}}), \kappa(Q_{\text{in}}), v_s(Q_{\text{in}}), A_\lambda(Q_{\text{in}}), A_\kappa(Q_{\text{in}}), m_s^2(Q_{\text{in}})\Big\}. \end{aligned} \tag{31}$$

Furthermore, an MSSM limit of the NMSSM can be defined by fixing the μ and the $B\mu$ parameters of the MSSM to their effective NMSSM values

$$\mu_{\text{eff}} := \frac{\lambda v_s}{\sqrt{2}}, \qquad B\mu_{\text{eff}} := \mu_{\text{eff}}\left(A_\lambda + \frac{\kappa v_s}{\sqrt{2}}\right), \tag{32}$$

and letting $\lambda, \kappa \to 0$. Accordingly, one has $v_s \to \infty$ and the new scalar gauge singlet s fully decouples from the Higgs sector.

4.2 Matching details

In the following we apply the `FlexibleEFTHiggs` method to the NMSSM. The matching of the NMSSM to the SM is performed analogously to Ref. [12], such that terms up to 3-loop order to $\hat{\lambda}_{\text{SM}}(Q_{\text{m}})$ are included, c.f. Eq. (6). At 1-loop level we include all NMSSM contributions, in particular all genuine NMSSM terms that dependend on λ and κ. At 2-loop level we take the MSSM-like terms of $\mathcal{O}\big(g_3^2(y_t^4 + y_b^4) + (y_t^2 + y_b^2)^3 + (y_t^2 + y_\tau^2)^3\big)$ into account in the gaugeless limit, $g_1 = g_2 = 0$, and in the zero-momentum approximation. This implies that NMSSM-specific terms are fully absent from $\Delta\lambda_{\text{SM}}^{2\ell}$. At 3-loop level we include the 3-loop QCD contributions of $\mathcal{O}\big(g_3^4 y_t^4\big)$ from Ref. [21].

4.3 Uncertainty estimation

The uncertainty estimation for the predicted light CP-even Higgs pole mass M_h in our `FlexibleEFTHiggs` NMSSM calculation is performed in an analogous way as in the MSSM, see Sect. 3.2. The total uncertainty is obtained via Eq. (18) from the combination of high-scale and low-scale

uncertainties. The low-scale uncertainty is identical to the one in the MSSM, and the high-scale uncertainty is defined via matching-scale variation as in Eq. (15). In this section, we discuss the NMSSM high-scale uncertainty. In particular, we focus on the question to what extent the matching scale variation is a reliable method to estimate missing NMSSM-specific higher-order terms that depend on λ and κ. The answer to this question is particularly important in parameter regions where these couplings are of $\mathcal{O}(1)$. In the following, we discuss this question in detail.

The analysis of the reliability of the matching scale variation below is performed according to the following strategy. First, the structure of missing NMSSM-specific terms contributing to $\hat{\lambda}_{\rm SM}(Q_{\rm m})$ up to 3-loop level is elaborated. Next, the structure of terms simulated by matching scale variation is derived. Since the matching scale is unphysical, the exact Higgs pole mass $M_h^{\rm exact}$ can not depend on it, whereas for the calculated Higgs mass M_h, the cancellation of the simulated matching scale-dependent higher-order terms is incomplete. The non-cancelled matching scale-dependent terms are the terms simulated by matching scale variation. Finally, the structure of the terms not included in $\hat{\lambda}_{\rm SM}(Q_{\rm m})$ is compared to the structure of the terms simulated by the matching scale variation. We will analyse to what extent the latter incorporates the former and in this way demonstrate the reliability of the high-scale uncertainty estimation.

We begin by focussing on missing NMSSM-specific corrections of 2-loop order and will then proceed to 3-loop. In any case, these corrections contribute to the SM quartic Higgs coupling $\hat{\lambda}_{\rm SM}(Q_{\rm m})$ and are eventually propagated to $\hat{\lambda}_{\rm SM}(Q_{\rm pole})$ at the low scale $Q_{\rm pole}$, thus affecting M_h^2. Analogously, NMSSM effects enter the other SM parameters. In this analysis, we work in the EFT limit ($v \ll M_S$) which is justified as we use a hybrid approach such that the EFT uncertainty can be expected to be negligibly small. Furthermore, we assume that the tree-level expression of $\hat{\lambda}^{0\ell}_{\rm SM}(Q_{\rm m})$ is of $\mathcal{O}\left(g_{1,2}^2 + (\lambda+\kappa)^2\right)$. We omit all terms containing the Yukawa couplings y_b and y_τ due to their small numerical impact. Also, we work in the gaugeless limit ($g_1 = g_2 = 0$). The only couplings remaining in this analysis are thus λ, κ, y_t and g_3.

In our calculation, the full NMSSM-specific 1-loop contributions are included. They exhibit the following structure:

$$\Delta\lambda^{1\ell}_{\rm SM}(Q_{\rm pole})\Big|_{\lambda,\kappa} = \kappa_L\Big[C^{1\ell}_{\lambda^4}\lambda^4 + C^{1\ell}_{\lambda^3\kappa}\lambda^3\kappa + \cdots + C^{1\ell}_{\kappa^5/\lambda}\frac{\kappa^5}{\lambda} + C^{1\ell}_{\kappa^6/\lambda^2}\frac{\kappa^6}{\lambda^2} + y_t^2\Big(C^{1\ell}_{y_t^2\lambda^2}\lambda^2 + C^{1\ell}_{y_t^2\lambda\kappa}\lambda\kappa + C^{1\ell}_{y_t^2\kappa^2}\kappa^2\Big)\Big], \tag{33}$$

where all $\overline{\rm DR}'$ parameters are expressed at the scale $Q_{\rm m}$. The coefficients $C^{n\ell}_{\cdots}$ and $\tilde{C}^{n\ell}_{\cdots}$ appearing in Eq. (33) and also hereafter are of $\mathcal{O}(1)$, by assuming the ratios $\mu_{\rm eff}/M_S$, A_λ/M_S and A_κ/M_S to be of the same order. It is noteworthy that λ also appears in the denominator due to Higgs couplings proportional to κv_s, where v_s is reexpressed in terms of λ and $\mu_{\rm eff}$ as $v_s = \sqrt{2}\mu_{\rm eff}/\lambda$, c.f. Eq. (23). By performing renormalization group running in the SM from $Q_{\rm m}$ down to $Q_{\rm low}$, all terms of leading and subleading order in large logarithms are fully resummed. Accordingly, at 2-loop level only NMSSM-specific terms that are free of large logarithms are missing in our calculation, corresponding to diagrams like the one given in Fig. 5a . These non-logarithmic 2-loop contributions are of the form

$$\begin{aligned}\Delta\lambda^{2\ell}_{\rm SM}(Q_{\rm pole})\Big|^{\rm miss}_{\lambda,\kappa} &= \kappa_L^2\Big[C^{2\ell}_{\lambda^6}\lambda^6 + C^{2\ell}_{\kappa\lambda^5}\lambda^5\kappa + \cdots + C^{2\ell}_{\kappa^9/\lambda^3}\frac{\kappa^9}{\lambda^3} + C^{2\ell}_{\kappa^{10}/\lambda^4}\frac{\kappa^{10}}{\lambda^4} + y_t^2\Big(C^{2\ell}_{y_t^2\lambda^4}\lambda^4 + C^{2\ell}_{y_t^2\lambda^3\kappa}\lambda^3\kappa + \cdots \\ &\quad + C^{2\ell}_{y_t^2\kappa^6/\lambda^2}\frac{\kappa^6}{\lambda^2}\Big) + y_t^2 g_3^2\Big(C^{2\ell}_{y_t^2 g_3^2\lambda^2}\lambda^2 + C^{2\ell}_{y_t^2 g_3^2\lambda\kappa}\lambda\kappa + C^{2\ell}_{y_t^2 g_3^2\kappa^2}\kappa^2\Big) \\ &\quad + y_t^4\Big(C^{2\ell}_{y_t^4\lambda^2}\lambda^2 + C^{2\ell}_{y_t^4\lambda\kappa}\lambda\kappa + C^{2\ell}_{y_t^4\kappa^2}\kappa^2\Big)\Big].\end{aligned} \tag{34}$$

At 3-loop level, the missing contributions include terms of first order in large logarithms, e.g. corresponding to diagrams shown in Fig. 5b , and non-logarithmic terms, e.g. corresponding to diagrams shown in Fig. 5c . These missing terms are thus of the form

$$\begin{aligned}\Delta\lambda^{3\ell}_{\rm SM}(Q_{\rm pole})\Big|^{\rm miss}_{\lambda,\kappa} &= \kappa_L^3\Big[\Big(\tilde{C}^{3\ell}_{\lambda^8}\lambda^8 + \cdots + \tilde{C}^{3\ell}_{\kappa^{14}/\lambda^6}\frac{\kappa^{14}}{\lambda^6}\Big) + y_t^2\Big(\tilde{C}^{3\ell}_{y_t^2\lambda^6}\lambda^6 + \cdots\Big) + y_t^2 g_3^2\Big(\tilde{C}^{3\ell}_{y_t^2 g_3^2\lambda^4}\lambda^4 + \cdots\Big) \\ &\quad + y_t^4\Big(\tilde{C}^{3\ell}_{y_t^4\lambda^4}\lambda^4 + \cdots\Big) + y_t^2 g_3^4\Big(\tilde{C}^{3\ell}_{y_t^2 g_3^4\lambda^2}\lambda^2 + \cdots\Big) \\ &\quad + y_t^4 g_3^2\Big(\tilde{C}^{3\ell}_{y_t^4 g_3^2\lambda^2}\lambda^2 + \cdots\Big) + y_t^6\Big(\tilde{C}^{3\ell}_{y_t^6\lambda^2}\lambda^2 + \cdots\Big)\Big]L \\ &\quad + \text{non-log-enhanced terms},\end{aligned} \tag{35}$$

wher e $L = \ln(Q_{\rm pole}/Q_{\rm m})$ represents a large logarithm and terms not enhanced by a large logarithm contain the same couplings structure as the logarithmically enhanced ones. The coeffcients of the latter are denoted by $\tilde{C}^{n\ell}_{\cdots}$ to distinguish them from the coefficients $C^{n\ell}_{\cdots}$ of the former ones.

In order to thoroughly work out the structure of the terms simulated by the variation of the matching scale, we shortly

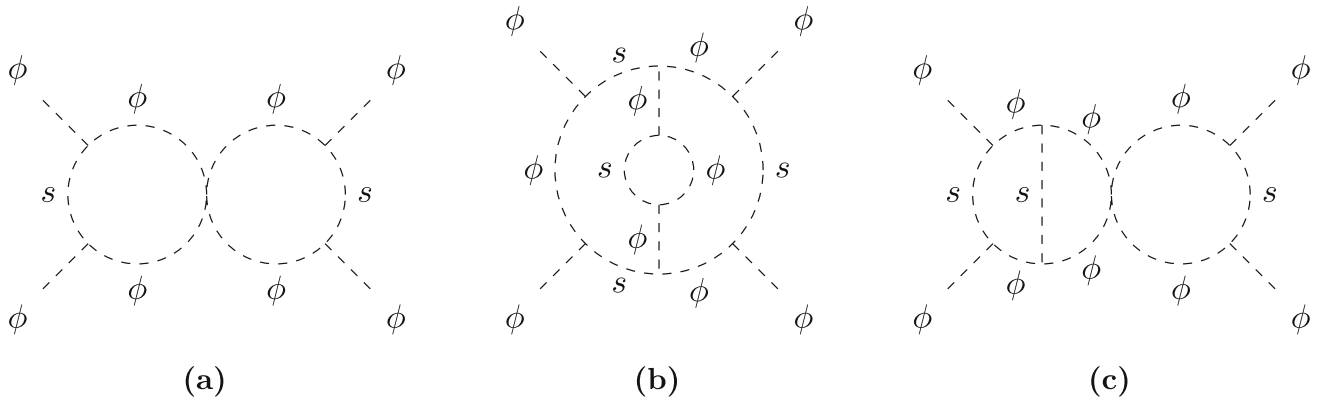

Fig. 5 Diagrams corresponding to contributions to $\hat{\lambda}_{\mathrm{SM}}(Q_{\mathrm{m}})$ not covered by the calculation, where $\phi \in \{\Re(h_u^0), \Re(h_d^0)\}$. a: non-log-enhanced 2-loop contribution of $\mathcal{O}\big((\lambda+\kappa)^4\lambda^2\big)$. b: log-enhanced 3-loop contribution of $\mathcal{O}\big((\lambda+\kappa)^8\big)$. c: non-log-enhanced 3-loop contribution of $\mathcal{O}\big((\lambda+\kappa)^6\lambda^2\big)$. Recall that triple scalar couplings involving one s contribute a vertex factor of $\mathcal{O}(\kappa+\lambda)$ and quartic vertices involving only ϕ a factor of $\mathcal{O}\big(\kappa^2/\lambda\big)$

recall some details of the procedure. We start this consideration with M_h^2 as the expression to be calculated in the SM using the $\overline{\mathrm{MS}}$ scheme at the renormalization scale Q_{pole},

$$M_h^2 = \hat{\lambda}_{\mathrm{SM}}\hat{v}^2 + \Delta M_h^{2,1\ell,\mathrm{SM}} + \Delta M_h^{2,2\ell,\mathrm{SM}} + \cdots . \tag{36}$$

The n-loop SM contributions $\Delta M_h^{2,n\ell,\mathrm{SM}}$ to M_h^2 depend on the SM $\overline{\mathrm{MS}}$ parameters $\hat{P}_{\mathrm{SM}}(Q_{\mathrm{pole}})$ from Eq. (5), all given at the scale Q_{pole}. Any SM parameter $\hat{p} \in \hat{P}_{\mathrm{SM}}(Q_{\mathrm{pole}})$ given at that scale[3] is obtained by performing renormalization group running down from the matching scale Q_{m}. The relation between a parameter $\hat{p} = \hat{p}(Q_{\mathrm{pole}})$ and its value $\hat{p}(Q_{\mathrm{m}})$ arises from the integration of the β function $\beta_{\hat{p}}$ via

$$\hat{p} = \hat{p}(Q_{\mathrm{m}}) - \int_{\ln Q_{\mathrm{pole}}}^{\ln Q_{\mathrm{m}}} \beta_{\hat{p}}(Q)\, \mathrm{d}(\ln Q). \tag{37}$$

The SM parameters at the renormalization scale Q_{m}, expressed in terms of NMSSM parameters $p \in P(Q_{\mathrm{m}})$ at that scale,[4] are obtained by using the matching relations of the form

$$\hat{p}(Q_{\mathrm{m}}) = \hat{p}^{0\ell}(p) + \Delta p^{1\ell}(p, Q_{\mathrm{m}}) + \cdots . \tag{38}$$

In this way, the value of $\hat{p}$ features an implicit dependence on the choice of Q_{m}. However, since the matching scale is an unphysical scale, $\hat{p}$ would not vary under changes in Q_{m} in an exact all-order calculation. In the `FlexibleEFTHiggs` calculation, a dependence on Q_{m} arises due to the truncation at a specific loop order. The following derivative is then a measure for the arising variation:

$$\frac{\mathrm{d}\hat{p}}{\mathrm{d}(\ln Q_{\mathrm{m}})} \overset{(37)}{=} \frac{\mathrm{d}\hat{p}(Q_{\mathrm{m}})}{\mathrm{d}(\ln Q_{\mathrm{m}})} - \beta_{\hat{p}}(Q_{\mathrm{m}}) \tag{39}$$

$$\overset{(38)}{=} \sum_p \frac{\partial \hat{p}^{0\ell}}{\partial p}\beta_p(Q_{\mathrm{m}}) + \sum_{k\geq 1}\left(\sum_p \frac{\partial \Delta p^{k\ell}}{\partial p}\beta_p(Q_{\mathrm{m}}) + \frac{\partial \Delta p^{k\ell}}{\partial(\ln Q_{\mathrm{m}})}\right) - \beta_{\hat{p}}(Q_{\mathrm{m}}). \tag{40}$$

The squared pole mass M_h^2, calculated by a truncated perturbation series, also depends upon Q_{m}, because it is obtained from the Q_{m}-dependent SM parameters. Via Eq. (36), an expression for the derivative of M_h^2 with respect to the matching scale can be found, connecting it to Eq. (40):

$$\frac{\mathrm{d}M_h^2}{\mathrm{d}(\ln Q_{\mathrm{m}})} = \sum_{\hat{p}} \frac{\partial}{\partial \hat{p}}\left(\hat{\lambda}_{\mathrm{SM}}\hat{v}^2 + \sum_{n\geq 1}\Delta M_h^{2,n\ell,\mathrm{SM}}\right)\frac{\mathrm{d}\hat{p}}{\mathrm{d}(\ln Q_{\mathrm{m}})}. \tag{41}$$

The expression in Eq. (41) is required to vanish when all orders are taken into account, as the physical Higgs pole mass must not depend on the matching scale.

In order for the matching scale variation to be an appropriate uncertainty estimation method, we demand the method to simulate all missing terms depending on λ and κ and therefore constituting NMSSM-specific terms, as mentioned above. To see whether this is indeed the case, we can explicitely evaluate Eq. (41) at the respective order in loops and couplings. At 2-loop level, we find in general at $\mathcal{O}(\mathcal{S})$, with $\mathcal{S}$ representing any relevant coupling structure:

[3] In the following we omit the renormalization scale from the SM $\overline{\mathrm{MS}}$ parameters $\hat{p} \in \hat{P}_{\mathrm{SM}}(Q_{\mathrm{pole}})$, if they are given at the scale Q_{pole}. We explicitely specify the scale, if it differs from Q_{pole}.

[4] In the following we omit the renormalization scale from the NMSSM $\overline{\mathrm{DR}}'$ parameters $p \in P(Q_{\mathrm{m}})$, if they are given at the scale Q_{m}. We explicitely specify the scale, if it differs from Q_{m}.

$$\left.\frac{\mathrm{d}M_h^2}{\mathrm{d}(\ln Q_\mathrm{m})}\right|_{\mathcal{S}} = \frac{\partial}{\partial\hat{\lambda}_\mathrm{SM}}\left(\hat{\lambda}_\mathrm{SM}\hat{v}^2+\mathcal{O}(\kappa_L)\right)$$
$$\left[\sum_p\left(\frac{\partial\hat{\lambda}^{0\ell}_\mathrm{SM}}{\partial p}\beta_p(Q_\mathrm{m})+\frac{\partial\Delta\lambda^{1\ell}_\mathrm{SM}}{\partial p}\beta_p(Q_\mathrm{m})\right)\right.$$
$$\left.+\frac{\partial\Delta\lambda^{1\ell}_\mathrm{SM}}{\partial(\ln Q_\mathrm{m})}+\underbrace{\frac{\partial\Delta\lambda^{2\ell}_\mathrm{SM}}{\partial(\ln Q_\mathrm{m})}}_{\text{incomplete}}-\beta_{\hat{\lambda}_\mathrm{SM}}(Q_\mathrm{m})+\mathcal{O}\left(\kappa_L^3\right)\right]\Big|_{\mathcal{S}}$$
$$+\frac{\partial}{\partial\hat{v}}\left(\hat{\lambda}_\mathrm{SM}\hat{v}^2+\mathcal{O}(\kappa_L)\right)$$
$$\left[\sum_p\left(\frac{\partial\hat{v}^{0\ell}}{\partial p}\beta_p(Q_\mathrm{m})+\frac{\partial\Delta v^{1\ell}}{\partial p}\beta_p(Q_\mathrm{m})\right)\right.$$
$$\left.+\frac{\partial\Delta v^{1\ell}}{\partial(\ln Q_\mathrm{m})}+\underbrace{\frac{\partial\Delta v^{2\ell}}{\partial(\ln Q_\mathrm{m})}}_{\text{incomplete}}-\beta_{\hat{v}}(Q_\mathrm{m})+\mathcal{O}\left(\kappa_L^3\right)\right]\Big|_{\mathcal{S}} \tag{42}$$

$$=-\left(v^2\frac{\partial\Delta\lambda^{2\ell}_\mathrm{SM}}{\partial(\ln Q_\mathrm{m})}\Big|^{\mathrm{miss}}+2\hat{\lambda}^{0\ell}_\mathrm{SM}v\frac{\partial\Delta v^{2\ell}}{\partial(\ln Q_\mathrm{m})}\Big|^{\mathrm{miss}}\right)\Big|_{\mathcal{S}}. \tag{43}$$

The terms above containing partial derivatives of $\Delta\lambda^{2\ell}_\mathrm{SM}$ and $\Delta v^{2\ell}$ with respect to $\ln Q_\mathrm{m}$ are incomplete in the performed `FlexibleEFTHiggs` calculation as their NMSSM-specific parts are omitted. However, their full inclusion would be necessary in order to ensure the complete cancellation of Q_m-dependent terms at $\mathcal{O}(\mathcal{S})$. The change in the Higgs mass under matching scale variation at that order therefore corresponds to the absent terms (denoted by "miss") in the way indicated in Eq. (43). Also, one can read off from Eq. (42) which present terms in the calculation of M_h^2 are the origin for simulated terms of $\mathcal{O}(\mathcal{S})$. These stem from the tree-level contribution as well as the 1-loop corrections to M_h^2 in the SM, incorporating logarithmic as well as non-logarithmic terms.

Equation (43) demonstrates that the logarithmic parts of the 2-loop matching correction to $\hat{\lambda}_\mathrm{SM}$ and $\hat{v}$ have to be analysed in order to clarify whether a specific needed coupling structure is generated during matching scale variation. This is the case if for the regarded order in the couplings, a matching contribution exists which also contains a logarithm of Q_m. We can elucidate that further by regarding the concrete example of the 2-loop contributions of $\mathcal{O}\left(\lambda^6v^2\right)$ to M_h^2. At that order, we yield:

$$\left.\frac{\mathrm{d}M_h^2}{\mathrm{d}(\ln Q_\mathrm{m})}\right|_{\lambda^6v^2} = -v^2\frac{\partial\Delta\lambda^{2\ell}_\mathrm{SM}}{\partial(\ln Q_\mathrm{m})}\Big|^{\mathrm{miss}}_{\lambda^6}-2\hat{\lambda}^{0\ell}_\mathrm{SM}\Big|_{\lambda^2}$$
$$v\frac{\partial\Delta v^{2\ell}}{\partial(\ln Q_\mathrm{m})}\Big|^{\mathrm{miss}}_{\lambda^4v}. \tag{44}$$

Since there are UV-divergent NMSSM-specific 2-loop corrections of $\mathcal{O}\left(\lambda^6\right)$ to the quartic self-interaction vertex of the SM-like Higgs, one can infer that logarithmic contributions to the 2-loop matching relation for $\hat{\lambda}_\mathrm{SM}$ enter at that order. With that, we can conclude that the maching scale variation generates 2-loop terms of $\mathcal{O}\left(\lambda^6v^2\right)$ in M_h^2, as they have a counterpart in the explicitely Q_m-dependent part of the 2-loop maching corrections $\Delta\lambda^{2\ell}_\mathrm{SM}$ and $\Delta v^{2\ell}$. Similar analyses for all other appearing NMSSM-specific coupling structures at 2-loop level lead to the same positive result. The matching scale variation can thus be deemed an appropriate method to estimate the uncertainty of the 2-loop `FlexibleEFTHiggs` calculation w.r.t. the missing NMSSM-specific terms.

At 3-loop level, a similar analysis can be applied. Here, we find an analogous result as at 2-loop level. In particular, missing terms enhanced by large logarithms L are generated by matching scale variation. This can be exemplified at $\mathcal{O}\left(\lambda^8v^2L\right)$ evaluating again Eq. (41) for this specific case:

$$\left.\frac{\mathrm{d}M_h^2}{\mathrm{d}(\ln Q_\mathrm{m})}\right|_{\lambda^8v^2L} = -\hat{v}^2\Big|_{\lambda^2v^2L}\frac{\partial\Delta\lambda^{2\ell}_\mathrm{SM}}{\partial(\ln Q_\mathrm{m})}\Big|^{\mathrm{miss}}_{\lambda^6}$$
$$-2\hat{\lambda}^{0\ell}_\mathrm{SM}\Big|_{\lambda^4L}v\frac{\partial\Delta v^{2\ell}}{\partial(\ln Q_\mathrm{m})}\Big|^{\mathrm{miss}}_{\lambda^4v}-2\hat{\lambda}^{0\ell}_\mathrm{SM}\Big|_{\lambda^2}\hat{v}\Big|_{\lambda^2L}\frac{\partial\Delta v^{2\ell}}{\partial(\ln Q_\mathrm{m})}\Big|^{\mathrm{miss}}_{\lambda^4v}. \tag{45}$$

Here, the large logarithm L appears due to the running of the SM parameters from Q_m to Q_pole by applying Eq. (37). The appearance of the large logarithm L corresponds to the fact that N^{2}LL terms of $\mathcal{O}\left(\lambda^8v^2\right)$ are not included in our calculation. The matching scale variation estimates these missing terms, though. Similarly, N^{2}LL terms of higher orders are covered as well.

From the outcomes of the presented analysis above, we infer that matching scale variation serves as a reliable mean for estimating the high-scale uncertainty of the calculated Higgs mass M_h^2. Especially, this is also true for the NMSSM-specific corrections entering the matching relations between the SM and the NMSSM.

4.4 Numerical results

In the following we present numerical results for the 3-loop `FlexibleEFTHiggs` calculation of the light CP-even Higgs boson pole mass M_h in NMSSM. In particular we study the impact of the NMSSM-specific couplings λ and κ on the predicted value of M_h. We furthermore inspect whether the λ- and κ-dependent uncertainties predominate against MSSM-like ones.

In our numerical study we set the NMSSM $\overline{\mathrm{DR}}'$ parameters to the values given in Eqs. (19a)–(19c), if not stated otherwise. The remaining NMSSM parameters, in particular $\lambda(Q_\mathrm{in})$, $\kappa(Q_\mathrm{in})$, $\mu_\mathrm{eff}(Q_\mathrm{in})$, $A_\lambda(Q_\mathrm{in})$ and $A_\kappa(Q_\mathrm{in})$ are set to

various values, depending on which specific kind of scenario is of interest.

4.4.1 Validation

In order to validate the newly implemented FlexibleEFTHiggs calculation in the NMSSM, we compare the obtained output with already existing results. These incorporate fixed-order (FO) and EFT calculations as well as FlexibleEFTHiggs results for the MSSM in FlexibleSUSY.

As a first test, the Higgs pole mass calculated in the MSSM limit of the NMSSM may be compared to the actual MSSM result based on the FlexibleEFTHiggs approach. For that comparison, we regard scenarios with degenerate SUSY mass parameters set to the common scale M_S. For the NMSSM, however, we make an exception concerning the mass-dimension parameters A_λ and A_κ in order to achieve accordance to the corresponding MSSM parameter point: A_λ is chosen such that $m_A = M_S$ is fulfilled. A_κ is then set to $A_\kappa = -|A_\lambda|$. In Fig. 6, the two curves corresponding to the MSSM Higgs mass and the NMSSM Higgs mass in the MSSM limit are given in both subfigures in dependence on M_S, clearly indicating a very good agreement. Also the estimated uncertainties indicate a stable calculation for $0.5\,\text{TeV} \leq M_S \leq 10\,\text{TeV}$, merely for $x_t = \sqrt{6}$ and $M_S \sim 1\,\text{TeV}$ jumps appear in the uncertainty caused by hierarchy transitions in Himalaya. A very similar picture arises in Fig. 7 where a very good agreement between the MSSM result and the NMSSM result in the MSSM limit was achieved and a nearly constant uncertainty was found, except for several in stabilities for $x_t \sim \sqrt{6}$ and for small M_S.

Next, a comparison with other NMSSM Higgs mass calculations also available in FlexibleSUSY is performed. The FlexibleEFTHiggs calculation, as it is now implemented in the model NMSSMEFTHiggs, allows to switch on and off the accessable 1-, 2- and 3-loop corrections to the $\hat{\lambda}_{\text{SM}}$-matching, as described in Sect. 4.2. These three options are denoted below as "FEFT $n\ell$", where n represents the highest loop-order of the corrections taken into account. Besides the hybrid FlexibleEFTHiggs calculation, also a fixed-order calculation in the NMSSM is available within FlexibleSUSY. That calculative approach has been implemented in the recently created model NUHNMSSMHimalaya. Similarly to the FlexibleEFTHiggs calculation, it allows to include MSSM-like 2-loop corrections of $\mathcal{O}\big(g_3^2(y_t^4+y_b^4)+(y_t^2+y_b^2)^3+(y_t^2)\,\mathcal{O}(+y_\tau^2)^3\big)$ to the Higgs mass as well as MSSM-like 3-loop corrections of $\mathcal{O}\big(g_3^4 y_t^4\big)$. If the latter ones are taken into account, it is denoted here as "FO 3ℓ", otherwise it is referred to as "FO 2ℓ".

In the left plot of Fig. 8 we compare the calculated Higgs pole mass in dependence on M_S obtained by the FlexibleEFTHiggs approach with the FO 2-loop and 3-loop results. There is a relatively good agreement between the four corresponding curves for $M_S < 1\,\text{TeV}$ as one would expect it for a comparison between hybrid and FO results. However, there is still a deviation of $\sim 1\,\text{GeV}$ for very low values of M_S, which originate from a different inclusion of terms of higher order between the two calculations. For larger SUSY scales, there are more significant deviations of the order $\sim 5\,\text{GeV}$, which can be explained by numerically important, log-enhanced terms of higher order, which are not included in the FO calculation at 2-loop and 3-loop level, respectively, but taken into account in the FlexibleEFTHiggs calculation. The broadening of the corresponding uncertainty band for increasing M_S mirrors this fact. However, the uncertainty for the FlexibleEFTHiggs -result remains nearly constant in the whole regarded scale range. Furthermore, the difference between the 2-loop and 3-loop FlexibleEFTHiggs results are remarkably small. These outcomes strongly suggest excellent convergence properties of the FlexibleEFTHiggs method.

In the right panel of Fig. 8, the dependence of M_h on x_t is shown. There, the differences between the results of the FlexibleEFTHiggs- and the FO-calculation are evident as well. Very remarkable is the significantly smaller width of the uncertainty band obtained with the FlexibleEFTHiggs calculation, in accordance with the findings above. FlexibleEFTHiggs- and 3-loop FO-results are separated by a gap of about 2 GeV, which is nearly independent of x_t. Also these observations indicate a much higher reliability of the FEFT-calculation.

Furthermore, a numerical comparison was carried out with the results from NMSSMCalc [13,70–72], which is based on a similar calculation including a hybrid approach with the option of choosing a Higgs pole mass matching. The corresponding result, obtained using pole mass matching with full 1-loop matching corrections and 2-loop corrections of $\mathcal{O}(\hat{g}_3^2\hat{y}_t^4+\hat{y}_t^6)$, is also shown in Fig. 8. The comparsion reveals a very good agreement between the two codes in general. The major difference to the 2-loop version of FlexibleEFTHiggs originates from the additional inclusion of 3-loop corrections in the relation between the top Yukawa coupling $\hat{y}_t$ and the top pole mass M_t which implies a nearly constant shift in M_h of about 0.5 GeV under variation of M_S and x_t, as Fig. 8 illustrates.[5] Further differences arise from the additional matching corrections involving the Yukawa couplings y_b and y_τ taken into account in FlexibleSUSY as well as from different choices of the parametrisation. While

[5] In order to trace back further origins of the difference, we internally applied a modification to the NMSSMCalc code to omit the 3-loop corrections to the top pole mass thanks to the support by Martin Gabelmann. The Higgs mass prediction obtained by the modified code is significantly closer to the FlexibleSUSY results. The difference is of the order of 0.3 GeV.

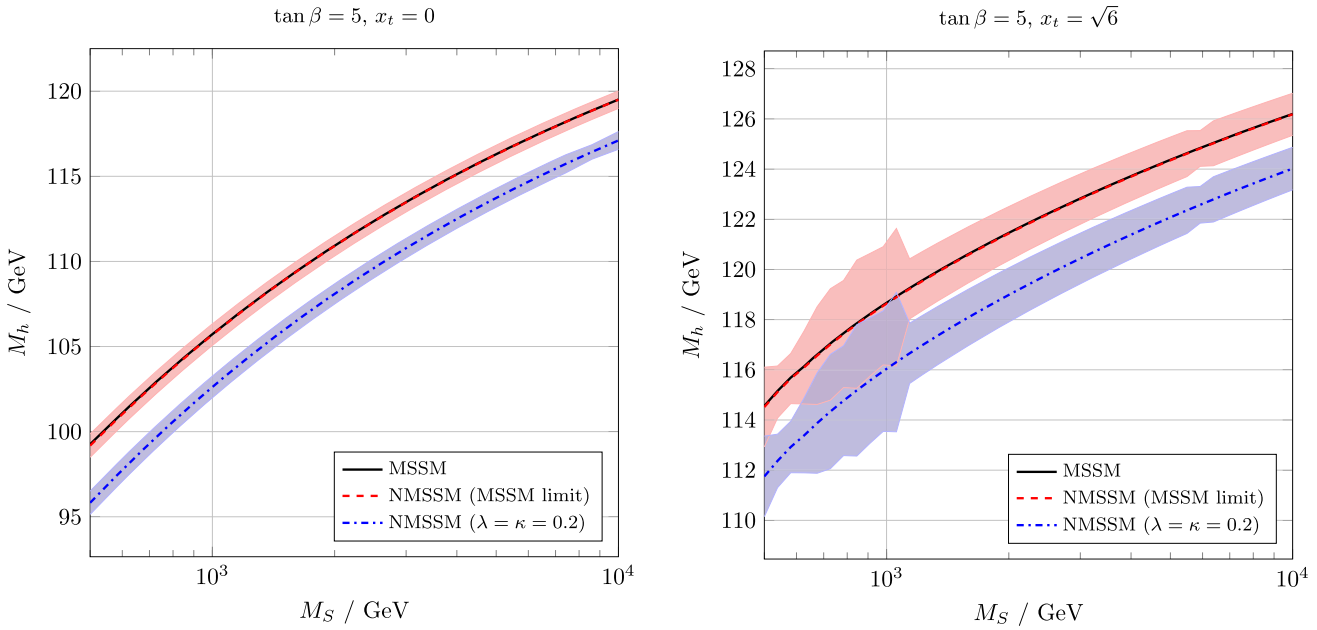

Fig. 6 Comparison between the calculated Higgs mass values in the MSSM and the NMSSM in dependence on M_S, obtained from the `FlexibleEFTHiggs` approach implemented in `FlexibleSUSY`. The left panel depicts the curves for $x_t = 0$ and the right one for $x_t = \sqrt{6}$. The red band represents the estimated uncertainty for the NMSSM calculation in the MSSM limit, while the blue band indicates the uncertainty for $\lambda = \kappa = 0.2$

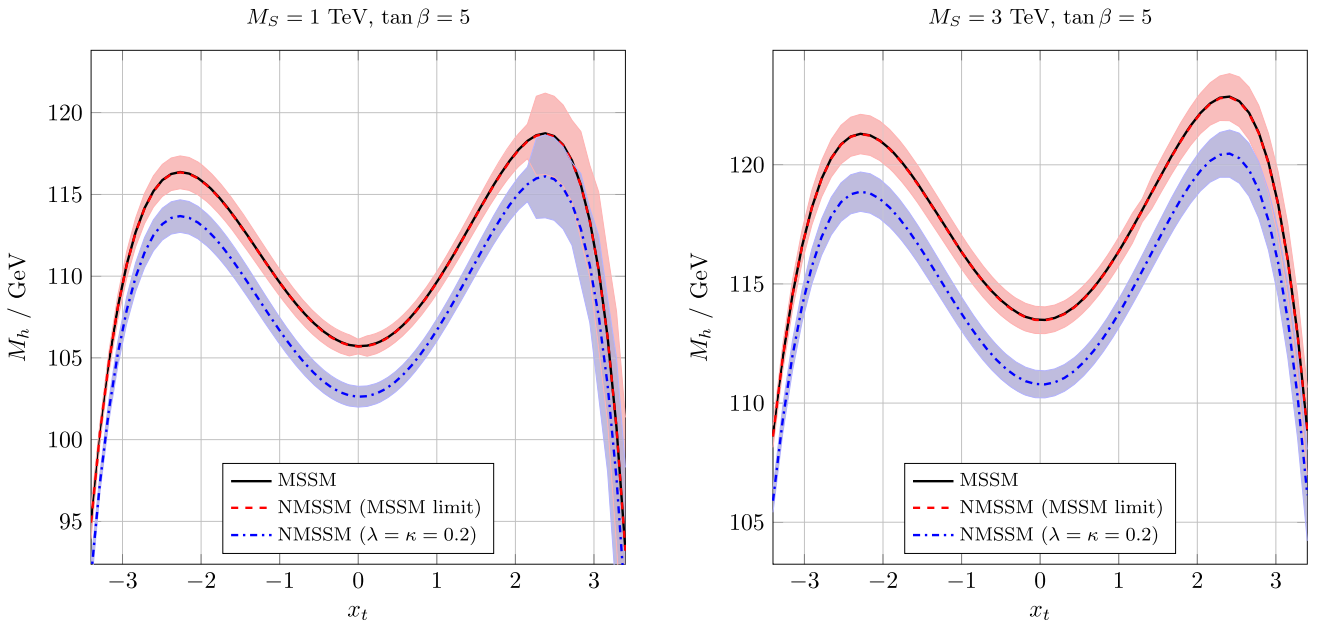

Fig. 7 Comparison between of the `FlexibleEFTHiggs` Higgs mass calculation in the MSSM and the NMSSM in dependence on x_t, in analogy to Fig. 6. The left panel depicts the curves for $M_S = 1$ TeV and the right one for $M_S = 3$ TeV

`NMSSMCalc` uses EFT parametrization, `FlexibleSUSY` uses full-model parametrization, leading to different higher-order terms in the high-scale matching including an effective resummation of terms involving x_t, see the discussion in Sec. 2 and Refs. [12,15]. Furthermore, `NMSSMCalc` differs in details of the low-scale matching between $\overline{\text{MS}}$ parameters and observables. Particularly in the algorithm for extracting the value of the top Yukawa coupling $\hat{y}_t$ from the top pole mass, different higher-order corrections are taken into account beyond the nominal accuracy.

Also, the results from Ref. [69] were compared to the `FlexibleSUSY` predictions. There, an EFT approach was

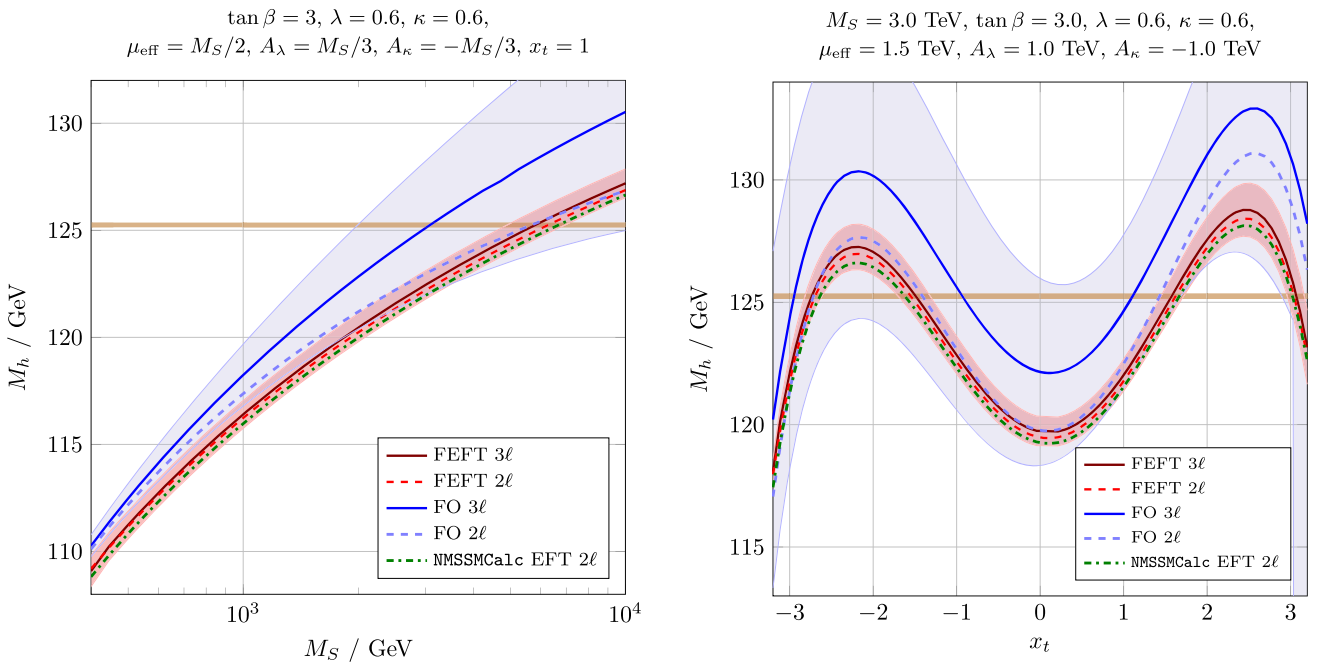

Fig. 8 Comparison between the calculated Higgs mass values obtained from different approaches implemented in `FlexibleSUSY`. The dependence $M_h(M_S)$ is shown on the left side, whereas $M_h(x_t)$ is shown on the right side. The red band represents the estimated uncertainty for the 3-loop `FlexibleEFTHiggs` calculation, while the blue band indicates the uncertainty for the 3-loop FO calculation. Additionally, the `NMSSMCalc` result obtained with pole mass matching including full 1-loop matching corrections and 2-loop corrections of $\mathcal{O}(\hat{g}_3^2\hat{y}_t^4 + \hat{y}_t^6)$ is plotted

applied including NMSSM-specific 2-loop QCD corrections to the matching. The comparison indicates a very good agreement as well. Additionally, it is worth mentioning that the study performed in Ref. [69] led to the conclusion that NMSSM-specific matching corrections contribute substantially only for quite large values of λ. This finding further corroborates the approach implemented in `FlexibleSUSY`.

4.4.2 NMSSM-specific effects

In this subsection, the behaviour and numerical impact of NMSSM-specific contributions to the SM-like Higgs pole mass M_h is analyzed. In particular, missing higher order terms of that kind are estimated based on the procedure presented in Sect. 4.3. They will also be compared to missing MSSM-like terms.

Figure 9 illustrates interplay of $\tan\beta$ and Yukawa couplings λ and κ in affecting Higgs pole mass M_h. The qualitative behaviour can be understood by considering the well-known dependence of the tree-level contribution on these two couplings. For large $\tan\beta$, the second term on the right side of Eq. (30) vanishes, while the non-vanishing third term leads to a negative shift which increases with growing $\lambda = \kappa$. For small $\tan\beta$ however, the second term dominates compared to the third one such that M_h increases with λ. Figure 9 thus demonstrates again, how strongly effects depending on λ and κ can influence M_h and accordingly their ability to alleviate the fine-tuning problem with regard to x_t in the MSSM.

The left plot in Fig. 10 shows the difference between M_h calculated at different matching loop orders in dependence on λ and κ, i.e. all precision settings were choosen as presented in appendix A with the corresponding value for flag 21 for each case. Here $M_h^{n\ell}$ denotes the Higgs pole mass calculated using n-loop matching. The curve representing the difference between $M_h^{0\ell}$ and $M_h^{1\ell}$ indicates large corrections and also a significant variation with $\lambda = \kappa$. In the MSSM-limit, one can read off that non-NMSSM-specific terms, originating mainly from top- and stop-contributions, lead to a shift of about -0.8 GeV. That difference considerably decreases in terms of absolute value when going to larger values of $\lambda = \kappa$ for the regarded parameter point, which thus demonstrates a strong dependence on these couplings. Considering the difference between $M_h^{2\ell}$ and $M_h^{1\ell}$, one recognises clearly less significant corrections below 1 GeV, only slightly depending on the two NMSSM-specific couplings. Similarly, one finds merely a mild dependence of $(M_h^{3\ell} - M_h^{2\ell})$, which however increases in its absolute value with respect to $(M_h^{2\ell} - M_h^{1\ell})$. As there is a sign change in the latter, this fact can be attributed to an accidental compensation of different contributions. All in all, this behaviour confirms the expectation of a good convergence of the perturbation series. It should however be kept in mind that NMSSM-specific 2-loop matching corrections

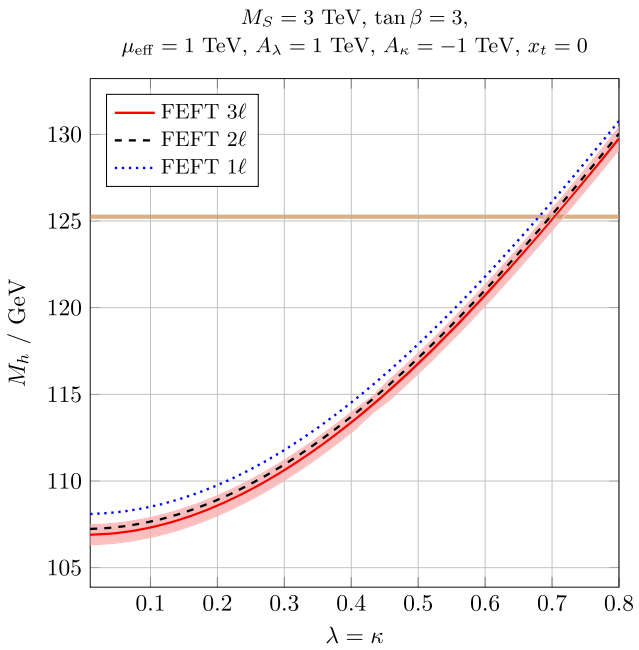

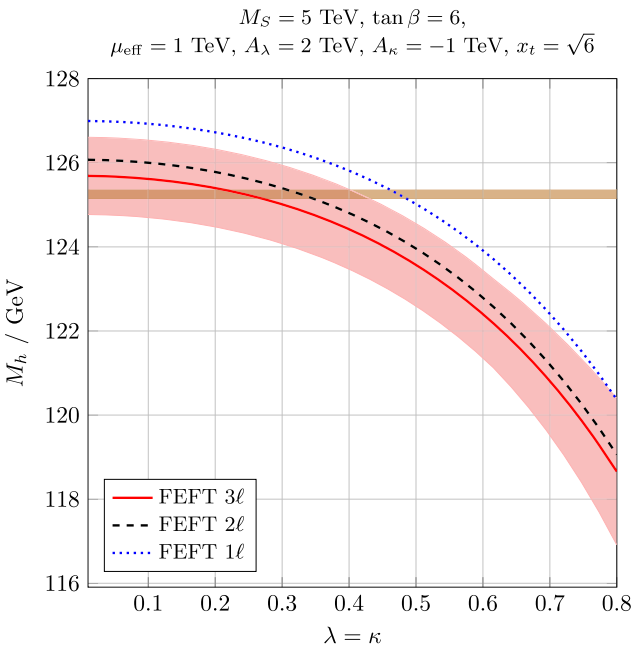

Fig. 9 Prediction of the Higgs pole mass M_h as calculated by the `FlexibleEFTHiggs` (FEFT) method at 1-, 2- and 3-loop precision in dependence on $\lambda = \kappa$ for different scenrios. The red curve represents the `FlexibleEFTHiggs` 3ℓ result, for which the red band indicates the estimated uncertainty. The horizontal brownish band marks again the experimentally determined value of M_h with its 1σ-uncertainty

are not included and are therefore not taken into account in the presented curve. In order to reassure that missing 2-loop and higher order terms in λ and κ do not spoil the precision of the calculation as suggested by the plot, a careful uncertainty estimation is essential.

The right panel of Fig. 10 indicates how the estimated uncertainty depends on λ and κ. For small couplings ($\lambda = \kappa < 0.2$), the uncertainty remains nearly constant at $\Delta M_h \sim 0.7\,\text{GeV}$. For $\tan\beta = 3$, a slight positive deviation appears in comparison to larger $\tan\beta$. However, the estimated uncertainty remains below 1 GeV there. In the range of moderate couplings, slight changes occur. While the uncertainty decreases with increasing λ and κ for $\tan\beta = 3$, it increases for larger considered values of $\tan\beta$. Beyond the perturbativity limit, the uncertaintes grow quickly. That tendency is stronger for larger $\tan\beta$. The plot thus indicates that for λ and κ allowed by the perturbativity limit, the uncertainties are of the order of $\sim 0.7\,\text{GeV}$ and only very slightly dependent on these couplings. In contrast, for values above that limit, there is a strong dependence entailing a significantly less reliable prediction of M_h. Also, comparing to the dependence of the uncertainty on x_t studied in Ref. [12], one comes to the conclusion that the variation of λ and κ below the perturbativity limit has only a minor numerical effect.

In order to substantiate the finding of an uncertainty of less than 1 GeV for scenarios with moderate $|x_t|$, a scan with $N = 10^3$ sample points was performed. The parameters were varied randomly in the following ranges:

$$1\,\text{TeV} \leq M_S \leq 10\,\text{TeV}, \qquad 2 \leq \tan\beta \leq 20, \tag{46a}$$

$$0.01 \leq \lambda, \kappa \leq 0.70, \qquad 200\,\text{GeV} \leq \mu_{\text{eff}} \leq 2500\,\text{GeV}, \tag{46b}$$

$$-2000\,\text{GeV} \leq A_\lambda \leq 5000\,\text{GeV}, \quad -2000\,\text{GeV} \leq A_\kappa \leq 0\,\text{GeV}, \tag{46c}$$

$$-\sqrt{6} \leq x_t \leq \sqrt{6}. \tag{46d}$$

During the scan, parameter choices leading to a wrong vacuum structure were ignored and generated anew. Among the points produced in this way, those violating the perturbativity limit for λ and κ were discarded. For each of the remaining 796 points, the theory uncertainty was estimated as described in the previous section. It was found that $\Delta M_h < 0.8\,\text{GeV}$ holds for 86.2% and $\Delta M_h < 1\,\text{GeV}$ for 97.9% of the parameter points. The majority of parameter points with higher uncertainties $\Delta M_h > 1\,\text{GeV}$ have large $|x_t|$. Nevertheless, even for large $|x_t|$ the typical uncertainty is small: out of the 144 points with $|x_t| > 2$ in the scan, 94% have $\Delta M_h < 1\,\text{GeV}$ GeV. Below, we will provide additional details on cases with large $|x_t|$.

4.4.3 Benchmark scenarios for M_h^{exp}

Next, some NMSSM benchmark scenarios are presented which reproduce the experimentally determined Higgs mass M_h within the 1σ-uncertainty band according to the 3-loop `FlexibleEFTHiggs` calculation as implemented in `FlexibleSUSY`. For the chosen points, the conditions from

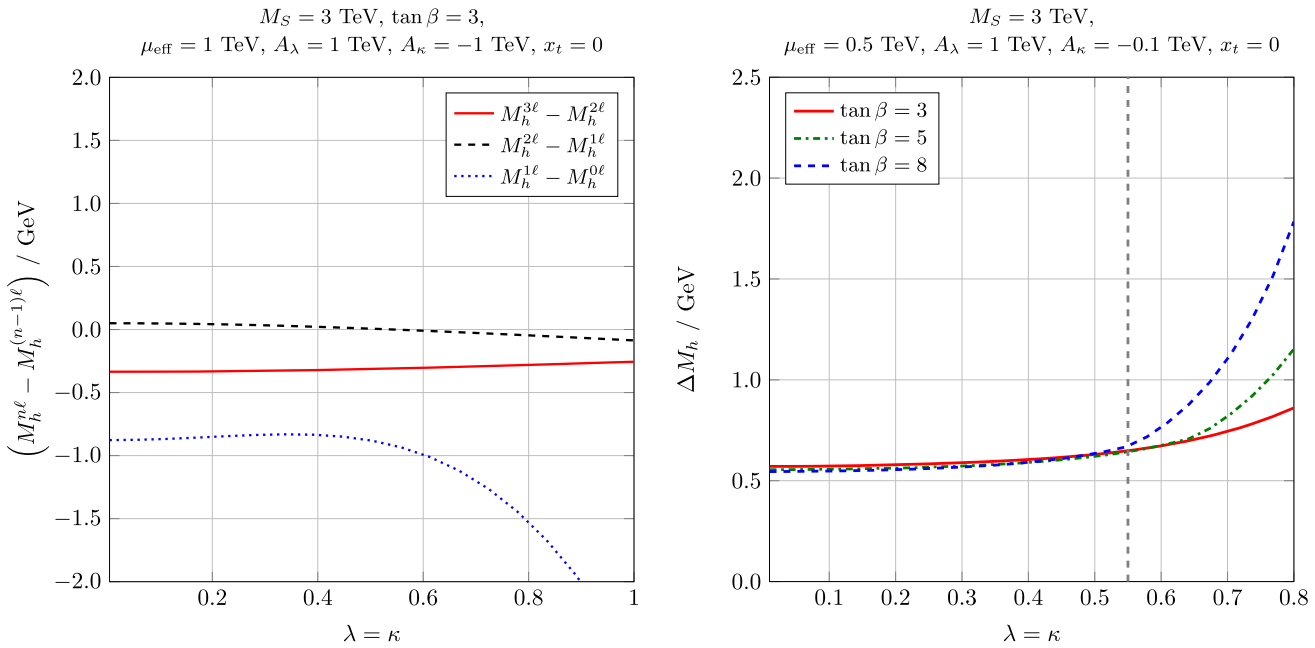

Fig. 10 On the left side, the differences between the Higgs masses calculated by using the `FlexibleEFTHiggs` approach with n-loop matching depending on λ and κ are shown. The dependence of the estimated theory uncertainty ΔM_h corresponding to missing higher order contributions for different values of $\tan\beta$ is depicted on the right side. Here, the vertical dashed line indicates the perturbativity limit, see Eq. (27)

Eqs. (19a)–(19c) are fulfilled again. The SUSY mass scale M_S is set to 3 TeV for each point. All other parameter are set as in Table 3.

The parameter values were chosen such that small, moderate and large values of $\tan\beta$ are covered (corresponding to the values 3, 7 and 20). In order to achieve a sufficiently high M_h, the NMSSM-specific couplings λ and κ are accordingly chosen to be small (~ 0.05) or large (~ 0.6) compared to the perturbativity limit. For each value of $\tan\beta$, one parameter point with a large mass splitting between the Higgs bosons and one point with a significantly smaller splitting were considered by adapting the value μ_{eff}. Finally, the remaining parameters were adjusted such that the experimental Higgs mass value is reproduced. Furthermore, one scenario was added with λ and κ beyond the perturbativity limit. The chosen set of points thus covers qualitatively very different situations that can occur within the NMSSM.

In Table 4 we show the Higgs mass spectra as obtained from `FlexibleSUSY` as well as the estimation of the uncertainties connected to missing higher order terms for the mass of the SM-like Higgs for the selected benchmark points. The values of the total uncertainty are each of the order 1 GeV, except for benchmark point S10 whose values for λ and κ are significantly beyond the perturbativity limit. This observation indicates again that the calculation presented here generates reliable results for various plausible scenarios within the NMSSM. The apparent fluctuation in the uncertainties can mostly be attributed to the different chosen values of μ_{eff} and x_t. The large uncertainty determined for S10 can however be directly ascribed to the large values of λ and κ, according to the findings of the previous subsection.

5 Summary and outlook

In this paper, we presented an analysis of the SM-like Higgs mass in the MSSM and its dependencies on various parameters, based on the implementation of the `FlexibleEFTHiggs` hybrid approach in `FlexibleSUSY`. The various scenarios regarded here are characterized by non-degenerated SUSY mass spectra, complementing the consideration of "standard" scenarios regarded in our previous study. In general, we found a very good reliability of the `FlexibleEFTHiggs` calculation for the large majority of the analysed cases according to the estimated theoretical uncertainty. The uncertainty is typically of the order of ~ 0.5 GeV. However, specific scenarios may lead to significantly higher uncertainties, especially ones that have a significant splitting in the third generation squark mass parameters.

We reported also about the most recent implementation of the `FlexibleEFTHiggs` calculation in the NMSSM, now publicly avaiable as a part of version 2.9.0 of `FlexibleSUSY`. It incorporates a treatment in the full-model parametrization as well as the inclusion of MSSM-like 2-loop and 3-loop contributions to the quartic SM Higgs coupling. This NMSSM hybrid calculation thus provides a Higgs

Table 3 Chosen parameter values for the analyzed benchmark points

BMP	$\tan\beta$	λ	κ	μ_{eff}/GeV	A_λ/GeV	A_κ/GeV	x_t
S1	20	0.05	0.05	800	1000	−500	1.85
S2	20	0.05	0.05	300	−250	−950	2.15
S4	7	0.30	0.30	800	5000	−100	2.05
S5	7	0.30	0.30	300	1200	−10	2.50
S7	3	0.60	0.30	750	2000	−1000	1.60
S8	3	0.55	0.35	300	700	−600	1.85
S10	3	1.50	1.50	800	250	−1000	0.25

Table 4 Calculated Higgs mass spectra for the benchmark points defined above. The estimated total uncertainty for the mass of the SM-like Higgs boson h_1 is also listed as well as its high-scale fraction. The low-scale uncertainty is nearly the same for all scenarios with about 0.3 GeV, its exact value can be calculated using Eq. (18). All masses and uncertainties are given in GeV

BMP	M_{h_1}	M_{h_2}	M_{h_3}	M_{A_1}	M_{A_2}	$M_{H^\pm}$	ΔM_{h_1}	$\Delta M_{h_1}^{\text{HS}}$
S1	125.17	1469.64	5346.08	1095.27	5346.12	5347.01	0.80	0.56
S2	125.11	274.45	433.03	432.72	924.38	441.98	0.60	0.36
S4	124.83	1574.00	5744.72	476.90	5745.17	5745.41	0.86	0.62
S5	125.16	590.79	1794.10	136.82	1793.29	1794.25	1.03	0.79
S7	125.37	451.88	2421.85	1070.46	2420.73	2418.73	0.68	0.44
S8	125.33	169.45	935.33	593.01	931.83	928.66	0.74	0.50
S10	125.11	1159.58	1612.76	1358.12	1625.07	1572.56	15.13	14.89

mass prediction at N^{3}LO with a resummation of large logarithms of N^{3}LL order in the respective couplings. In this way, significant progress is achieved in comparison to the previous implementation of the `FlexibleEFTHiggs` method for the NMSSM in `FlexibleSUSY`. The results obtained from applying the calculation to several different scenarios indicate a high stability of the code. In general, the 3-loop SUSY QCD contributions have a rather small impact on the Higgs mass, e.g. of the order of 0.1 GeV for degenerate mass spectra with $M_S \approx 3$ TeV. However, the 3-loop calculation can suffer from large uncertainties and discontinuities due to hierarchy transitions which might be problematic in some applications. Therefore we recommend to use the 2-loop calculation when the 3-loop calculation leads to significantly larger uncertainties or if continuity of the Higgs mass prediction is required.

The reliability of the Higgs pole mass calculation in the NMSSM has been further corroborated by studying the potential impact of NMSSM-specific missing higher-order terms. It was confirmed that matching scale variation is an appropriate means to simulate the effect of those disregarded contributions, unless very specific conditions are fulfilled, like $\kappa \gg \lambda$. The theoretical uncertainty was found to be nearly constant all over the parameter space allowed by the perturbativity limit on λ and κ with $\Delta M_h \approx 0.7$ GeV, making it one of the most precise calculations of the SM-like Higgs boson mass in the NMSSM currently available.

Acknowledgements We thank the `NMSSMCalc` developers and in particular M. Gabelmann for supporting the comparison to `FlexibleSUSY` and the clarification the differences between the two codes. This research was supported by the German Research Foundation (DFG) under grant number STO 876/2-3 and by the high-performance computing cluster Taurus at ZIH, TU Dresden.

Data availability statement Data will be made available on reasonable request. [Authors' comment: The datasets generated during and/or analysed during the current study are available from the corresponding author on reasonable request.]

Code availability statement This manuscript has associated code/software in a data repository. [Authors' comment: The code/software generated during and/or analysed during the current study is available in the FlexibleSUSY repository, https://github.com/FlexibleSUSY/FlexibleSUSY.]

Open Access This article is licensed under a Creative Commons Attribution 4.0 International License, which permits use, sharing, adaptation, distribution and reproduction in any medium or format, as long as you give appropriate credit to the original author(s) and the source, provide a link to the Creative Commons licence, and indicate if changes were made. The images or other third party material in this article are included in the article's Creative Commons licence, unless indicated otherwise in a credit line to the material. If material is not included in the article's Creative Commons licence and your intended use is not permitted by statutory regulation or exceeds the permitted use, you will need to obtain permission directly from the copyright holder. To view a copy of this licence, visit http://creativecommons.org/licenses/by/4.0/.
Funded by SCOAP^3.

A SUSY Les Houches input

The SUSY Les Houches (SLHA) input file for FlexibleSUSY's NMSSMEFTHiggs model used for the benchmark point S1 is given below. The precision settings for all other 3-loop FlexibleEFTHiggs calculations presented in this publication are chosen identical.

For the 2-loop FlexibleEFTHiggs calculations performed in this work the flag 21 in the FlexibleSUSY block is set to 2 and analogously for the 1-loop calculations.

```
Block FlexibleSUSY
0    1.0e-05     # precision goal
1    0           # max. iterations
                  (0 = automatic)
2    0           # algorithm (0 = all, 1 = two_scale, 2 = semi_analytic)
3    0           # calculate SM pole masses
4    3           # pole mass loop order
5    3           # EWSB loop order
6    4           # beta-functions loop order
7    3           # threshold corrections loop order
8    1           # Higgs 2-loop corrections O(alpha_t alpha_s)
9    1           # Higgs 2-loop corrections O(alpha_b alpha_s)
10    1           # Higgs 2-loop corrections O((alpha_t + alpha_b)^2)
11    1           # Higgs 2-loop corrections O(alpha_tau^2)
12    0           # force output
13    2           # Top pole mass QCD corrections (0 = 1L, 1 = 2L, 2 = 3L, 3 = 4L)
14    1.0e-11     # beta-function zero threshold
15    0           # calculate all observables
16    0           # force positive majorana masses
17    0           # pole mass renormalization scale (0 = SUSY scale)
18    0           # pole mass renormalization scale in the EFT (0 = min(SUSY \
  scale, Mt))
19    0           # EFT matching scale (0 = SUSY scale)
20    2           # EFT loop order for upwards matching
21    3           # EFT loop order for downwards matching
22    0           # EFT index of SM-like Higgs in the BSM model
23    1           # calculate BSM pole masses
24    124111321   # individual threshold correction loop orders
25    0           # ren. scheme for Higgs 3L corrections (0 = DR, 1 = MDR)
26    1           # Higgs 3-loop corrections O(alpha_t alpha_s^2)
27    0           # Higgs 3-loop corrections O(alpha_b alpha_s^2)
28    0           # Higgs 3-loop corrections O(alpha_t^2 alpha_s)
29    0           # Higgs 3-loop corrections O(alpha_t^3)
30    0           # Higgs 4-loop corrections O(alpha_t alpha_s^3)
31    0           # loop library (0 = softsusy)
Block SMINPUTS          # Standard Model inputs
1    1.279160000e+02    # alpha^(-1) SM MSbar(MZ)
2    1.166378700e-05    # G_Fermi
3    1.184000000e-01    # alpha_s(MZ) SM MSbar
4    9.118760000e+01    # MZ(pole)
5    4.18000000e+00     # mb(mb) SM MSbar
6    1.73340000e+02     # mtop(pole)
7    1.77700000e+00     # mtau(pole)
8    0.00000000e+00     # mnu3(pole)
9    80.384             # MW pole
11    5.10998902e-04     # melectron(pole)
12    0.00000000e+00     # mnu1(pole)
13    1.05658357e-01     # mmuon(pole)
14    0.00000000e+00     # mnu2(pole)
21    4.75000000e-03     # md(2 GeV) MS-bar
22    2.40000000e-03     # mu(2 GeV) MS-bar
23    1.04000000e-01     # ms(2 GeV) MS-bar
24    1.27000000e+00     # mc(mc) MS-bar
```

```
Block EXTPAR
0    3000    # MSUSY
1    3000    # M1
2    3000    # M2
3    3000    # M3
4    3000    # Mu
25   20      # TanBeta
61   0.05    # Lambda
62   0.05    # Kappa
63   1000    # ALambda
64  -500     # AKappa
Block MSQ2IN
1  1      9.0e+06    # mq2(1,1)
2  2      9.0e+06    # mq2(2,2)
3  3      9.0e+06    # mq2(3,3)
Block MSE2IN
1  1      9.0e+06    # me2(1,1)
2  2      9.0e+06    # me2(2,2)
3  3      9.0e+06    # me2(3,3)
Block MSL2IN
1  1      9.0e+06    # ml2(1,1)
2  2      9.0e+06    # ml2(2,2)
3  3      9.0e+06    # ml2(3,3)
Block MSU2IN
1  1      9.0e+06    # mu2(1,1)
2  2      9.0e+06    # mu2(2,2)
3  3      9.0e+06    # mu2(3,3)
Block MSD2IN
1  1      9.0e+06    # md2(1,1)
2  2      9.0e+06    # md2(2,2)
3  3      9.0e+06    # md2(3,3)
Block AUIN
1  1      0    # Au(1,1)
2  2      0    # Au(2,2)
3  3   5590    # Au(3,3)
Block ADIN
1  1      0    # Ad(1,1)
2  2      0    # Ad(2,2)
3  3      0    # Ad(3,3)
Block AEIN
1  1      0    # Ad(1,1)
2  2      0    # Ad(2,2)
3  3      0    # Ad(3,3)
```

References

1. G. Aad et al., Observation of a new particle in the search for the Standard Model Higgs boson with the ATLAS detector at the LHC. Phys. Lett. B **716**, 1–29 (2012). https://doi.org/10.1016/j.physletb.2012.08.020
2. S. Chatrchyan et al., Observation of a new boson at a mass of 125 GeV with the CMS Experiment at the LHC. Phys. Lett. B **716**, 30–61 (2012). https://doi.org/10.1016/j.physletb.2012.08.021
3. P. Slavich et al., Higgs-mass predictions in the MSSM and beyond. Eur. Phys. J. C **81**, 5 (2021). https://doi.org/10.1140/epjc/s10052-021-09198-2. Ed. by P. Slavich and S. Heinemeyer, p. 450
4. T. Hahn et al., High-precision predictions for the light CP-even Higgs boson mass of the minimal supersymmetric standard model. Phys. Rev. Lett. **112**(14), 141801 (2014). https://doi.org/10.1103/PhysRevLett.112.141801
5. H. Bahl, W. Hollik, Precise prediction for the light MSSM Higgs boson mass combining effective field theory and fixed-order calculations. Eur. Phys. J. C **76**(9), 499 (2016). https://doi.org/10.1140/epjc/s10052-016-4354-8
6. F. Staub, W. Porod, Improved predictions for intermediate and heavy supersymmetry in the MSSM and beyond. Eur. Phys. J. C **77**(5), 338 (2017). https://doi.org/10.1140/epjc/s10052-017-4893-7
7. H. Bahl, W. Hollik, Precise prediction of the MSSM Higgs boson masses for low M_A. JHEP **07**, 182 (2018). https://doi.org/10.1007/JHEP07(2018)182
8. H. Bahl, I. Sobolev, G. Weiglein, The light MSSM Higgs boson mass for large tan β and complex input parameters. Eur. Phys. J. C **80**(11), 1063 (2020). https://doi.org/10.1140/epjc/s10052-020-08637-w
9. H. Bahl, N. Murphy, H. Rzehak, Hybrid calculation of the MSSM Higgs boson masses using the complex THDM as EFT. Eur. Phys. J. C **81**(2), 128 (2021). https://doi.org/10.1140/epjc/s10052-021-08939-7

10. P. Athron et al., Precise Higgs mass calculations in (non-)minimal supersymmetry at both high and low scales. JHEP **01**, 079 (2017). https://doi.org/10.1007/JHEP01(2017)079
11. P. Athron et al., FlexibleSUSY 2.0: Extensions to investigate the phenomenology of SUSY and non-SUSY models. Comput. Phys. Commun. **230**, 145–217 (2018). https://doi.org/10.1016/j.cpc.2018.04.016
12. T. Kwasnitza, D. Stöckinger, A. Voigt, Improved MSSM Higgs mass calculation using the 3-loop FlexibleEFTHiggs approach including x_t-resummation. JHEP **07**(07), 197 (2020). https://doi.org/10.1007/JHEP06(2023)201
13. C. Borschensky et al., Higgs mass predictions in the CP-violating high-scale NMSSM. Eur. Phys. J. C **85**(2), 168 (2025). https://doi.org/10.1140/epjc/s10052-024-13723-4
14. P. Athron et al., FlexibleSUSY – a spectrum generator generator for supersymmetric models. Comput. Phys. Commun. **190**, 139–172 (2015). https://doi.org/10.1016/j.cpc.2014.12.020
15. T. Kwasnitza, D. Stöckinger, Resummation of terms enhanced by trilinear squark-Higgs couplings in the MSSM. JHEP **08**, 070 (2021). https://doi.org/10.1007/JHEP08(2021)070
16. S. Borowka, S. Paßehr, G. Weiglein, Complete two-loop QCD contributions to the lightest Higgs-boson mass in the MSSM with complex parameters. Eur. Phys. J. C **78**(7), 576 (2018). https://doi.org/10.1140/epjc/s10052-018-6055-y
17. E. Bagnaschi et al., Full two-loop QCD corrections to the Higgs mass in the MSSM with heavy superpartners. Eur. Phys. J. C **79**(11), 910 (2019). https://doi.org/10.1140/epjc/s10052-019-7417-9
18. D. Meuser, Complete electroweak $\mathcal{O}({N_c}^2)$ two-loop contributions to the Higgs boson masses in the MSSM and aspects of two-loop renormalisation. PhD thesis. Hamburg: Hamburg U., 2023. https://doi.org/10.3204/PUBDB-2024-05606
19. H. Bahl, D. Meuser, G. Weiglein, Complete electroweak $\mathcal{O}\left({N_c}^2\right)$ two-loop contributions to the Higgs boson masses in the MSSM and aspects of two-loop renormalisation. Eur. Phys. J. C **84**(10), 1017 (2024). https://doi.org/10.1140/epjc/s10052-024-13379-0
20. R.V. Harlander, J. Klappert, A. Voigt, Higgs mass prediction in the MSSM at three-loop level in a pure $\overline{\text{DR}}$ context. Eur. Phys. J. C **77**(12), 814 (2017). https://doi.org/10.1140/epjc/s10052-017-5368-6
21. R.V. Harlander et al., The light CP-even MSSM Higgs mass resummed to fourth logarithmic order. Eur. Phys. J. C **78**(10), 874 (2018). https://doi.org/10.1140/epjc/s10052-018-6351-6
22. P. Kant et al., Light MSSM Higgs boson mass to three-loop accuracy. JHEP **08**, 104 (2010). https://doi.org/10.1007/JHEP08(2010)104
23. I. Jack et al., Decoupling of the epsilon scalar mass in softly broken supersymmetry. Phys. Rev. D **50**, R5481–R5483 (1994). https://doi.org/10.1103/PhysRevD.50.R5481
24. D.R.T. Jones, Asymptotic behavior of supersymmetric Yang–Mills theories in the two loop approximation. Nucl. Phys. B **87**, 127 (1975). https://doi.org/10.1016/0550-3213(75)90256-4
25. D.R.T. Jones, L. Mezincescu, The beta function in supersymmetric Yang–Mills theory. Phys. Lett. B **136**, 242–244 (1984). https://doi.org/10.1016/0370-2693(84)91154-7
26. P.C. West, The Yukawa beta function in N=1 rigid supersymmetric theories. Phys. Lett. B **137**, 371–373 (1984). https://doi.org/10.1016/0370-2693(84)91734-9
27. S.P. Martin, M.T. Vaughn, Regularization dependence of running couplings in softly broken supersymmetry. Phys. Lett. B **318**, 331–337 (1993). https://doi.org/10.1016/0370-2693(93)90136-6
28. Y. Yamada, Two loop renormalization of gaugino masses in general supersymmetric gauge models. Phys. Rev. Lett. **72**, 25–27 (1994). https://doi.org/10.1103/PhysRevLett.72.25
29. I. Jack, D.R.T. Jones, Soft supersymmetry breaking and finiteness. Phys. Lett. B **333**, 372–379 (1994). https://doi.org/10.1016/0370-2693(94)90156-2
30. Y. Yamada, Two loop renormalization group equations for soft SUSY breaking scalar interactions: supergraph method. Phys. Rev. D **50**, 3537–3545 (1994). https://doi.org/10.1103/PhysRevD.50.3537
31. S.P. Martin, M.T. Vaughn, Two loop renormalization group equations for soft supersymmetry breaking couplings. Phys. Rev. D **50**, 2282 (1994). https://doi.org/10.1103/PhysRevD.50.2282. [Erratum: Phys. Rev. D 78, 039903 (2008)]
32. R.M. Fonseca et al., Running soft parameters in SUSY models with multiple U(1) gauge factors. Nucl. Phys. B **854**, 28–53 (2012). https://doi.org/10.1016/j.nuclphysb.2011.08.017
33. M.D. Goodsell, Two-loop RGEs with Dirac gaugino masses. JHEP **01**, 066 (2013). https://doi.org/10.1007/JHEP01(2013)066
34. M. Sperling, D. Stöckinger, A. Voigt, Renormalization of vacuum expectation values in spontaneously broken gauge theories. JHEP **07**, 132 (2013). https://doi.org/10.1007/JHEP07(2013)132
35. M. Sperling, D. Stöckinger, A. Voigt, Renormalization of vacuum expectation values in spontaneously broken gauge theories: two-loop results. JHEP **01**, 068 (2014). https://doi.org/10.1007/JHEP01(2014)068
36. I. Jack, D.R.T. Jones, A.F. Kord, Three loop soft running, benchmark points and semiperturbative unification. Phys. Lett. B **579**, 180–188 (2004). https://doi.org/10.1016/j.physletb.2003.10.083
37. I. Jack, D.R.T. Jones, A.F. Kord, Snowmass benchmark points and three-loop running. Ann. Phys. **316**, 213–233 (2005). https://doi.org/10.1016/j.aop.2004.08.007
38. G. Degrassi, P. Slavich, F. Zwirner, On the neutral Higgs boson masses in the MSSM for arbitrary stop mixing. Nucl. Phys. B **611**, 403–422 (2001). https://doi.org/10.1016/S0550-3213(01)00343-1
39. A. Brignole et al., On the O(alpha(t)**2) two loop corrections to the neutral Higgs boson masses in the MSSM. Nucl. Phys. B **631**, 195–218 (2002). https://doi.org/10.1016/S0550-3213(02)00184-0
40. A. Dedes, P. Slavich, Two loop corrections to radiative electroweak symmetry breaking in the MSSM. Nucl. Phys. B **657**, 333–354 (2003). https://doi.org/10.1016/S0550-3213(03)00173-1
41. A. Brignole et al., On the two loop sbottom corrections to the neutral Higgs boson masses in the MSSM. Nucl. Phys. B **643**, 79–92 (2002). https://doi.org/10.1016/S0550-3213(02)00748-4
42. A. Dedes, G. Degrassi, P. Slavich, On the two loop Yukawa corrections to the MSSM Higgs boson masses at large tan beta. Nucl. Phys. B **672**, 144–162 (2003). https://doi.org/10.1016/j.nuclphysb.2003.08.033
43. J.P. Vega, G. Villadoro, SusyHD: Higgs mass determination in supersymmetry. JHEP **07**, 159 (2015). https://doi.org/10.1007/JHEP07(2015)159
44. L.N. Mihaila, J. Salomon, M. Steinhauser, Gauge coupling beta functions in the standard model to three loops. Phys. Rev. Lett. **108**, 151602 (2012). https://doi.org/10.1103/PhysRevLett.108.151602
45. A.V. Bednyakov, A.F. Pikelner, V.N. Velizhanin, Anomalous dimensions of gauge fields and gauge coupling beta-functions in the Standard Model at three loops. JHEP **01**, 017 (2013). https://doi.org/10.1007/JHEP01(2013)017
46. A.V. Bednyakov, A.F. Pikelner, V.N. Velizhanin, Yukawa coupling beta-functions in the Standard Model at three loops. Phys. Lett. B **722**, 336–340 (2013). https://doi.org/10.1016/j.physletb.2013.04.038
47. K.G. Chetyrkin, M.F. Zoller, Three-loop β-functions for top-Yukawa and the Higgs self-interaction in the Standard Model. JHEP **06**, 033 (2012). https://doi.org/10.1007/JHEP06(2012)033
48. A.V. Bednyakov, A.F. Pikelner, V.N. Velizhanin, Higgs self-coupling beta-function in the Standard Model at three loops. Nucl. Phys. B **875**, 552–565 (2013). https://doi.org/10.1016/j.nuclphysb.2013.07.015
49. K.G. Chetyrkin, M.F. Zoller, Leading QCD-induced four-loop contributions to the β -function of the Higgs self-coupling in the

SM and vacuum stability. JHEP **06**, 175 (2016). https://doi.org/10.1007/JHEP06(2016)175
50. S.P. Martin, Four-loop Standard Model effective potential at leading order in QCD. Phys. Rev. D **92**(5), 054029 (2015). https://doi.org/10.1103/PhysRevD.92.054029
51. A.V. Bednyakov, A.F. Pikelner, Four-loop strong coupling beta-function in the Standard Model. Phys. Lett. B **762**, 151–156 (2016). https://doi.org/10.1016/j.physletb.2016.09.007
52. G. Degrassi et al., Higgs mass and vacuum stability in the Standard Model at NNLO. JHEP **08**, 098 (2012). https://doi.org/10.1007/JHEP08(2012)098
53. S.P. Martin, D.G. Robertson, Higgs boson mass in the Standard Model at two-loop order and beyond. Phys. Rev. D **90**(7), 073010 (2014). https://doi.org/10.1103/PhysRevD.90.073010
54. R.V. Harlander, J. Klappert, A. Voigt, The light CP-even MSSM Higgs mass including N^3LO+N^3LL QCD corrections. Eur. Phys. J. C **80**(3), 186 (2020). https://doi.org/10.1140/epjc/s10052-020-7747-7
55. E. Bagnaschi et al., Higgs mass and unnatural supersymmetry. JHEP **09**, 092 (2014). https://doi.org/10.1007/JHEP09(2014)092
56. B.C. Allanach, A. Voigt, Uncertainties in the lightest CP even Higgs boson mass prediction in the minimal supersymmetric Standard Model: fixed order versus effective field theory prediction. Eur. Phys. J. C **78**(7), 573 (2018). https://doi.org/10.1140/epjc/s10052-018-6046-z
57. H. Bahl et al., Theoretical uncertainties in the MSSM Higgs boson mass calculation. Eur. Phys. J. C **80**(6), 497 (2020). https://doi.org/10.1140/epjc/s10052-020-8079-3
58. H. Bahl, I. Sobolev, G. Weiglein, Precise prediction for the mass of the light MSSM Higgs boson for the case of a heavy gluino. Phys. Lett. B **808**, 135644 (2020). https://doi.org/10.1016/j.physletb.2020.135644
59. S.P. Martin, Top-quark pole mass in the tadpole-free $\overline{MS}$ scheme. Phys. Rev. D **93**(9), 094017 (2016). https://doi.org/10.1103/PhysRevD.93.094017
60. S. Navas et al., Review of particle physics. Phys. Rev. D **110**(3), 030001 (2024). https://doi.org/10.1103/PhysRevD.110.030001
61. P.H. Chankowski, S. Pokorski, J. Rosiek, Complete on-shell renormalization scheme for the minimal supersymmetric Higgs sector. Nucl. Phys. B **423**, 437–496 (1994). https://doi.org/10.1016/0550-3213(94)90141-4
62. A. Dabelstein, The one loop renormalization of the MSSM Higgs sector and its application to the neutral scalar Higgs masses. Z. Phys. C **67**, 495–512 (1995). https://doi.org/10.1007/BF01624592
63. M. Carena et al., Analytical expressions for radiatively corrected Higgs masses and couplings in the MSSM. Phys. Lett. B **355**, 209–221 (1995). https://doi.org/10.1016/0370-2693(95)00694-G
64. S. Heinemeyer, W. Hollik, G. Weiglein, The masses of the neutral CP-even Higgs bosons in the MSSM: accurate analysis at the two loop level. Eur. Phys. J. C **9**, 343–366 (1999). https://doi.org/10.1007/s100529900006
65. N .Polonsky, The Mu parameter of supersymmetry. In: International Symposium on Supersymmetry, Supergravity and Superstring, pp. 100–124 (1999)
66. K.J. Bae et al., Revisiting the SUSY μ problem and its solutions in the LHC era. Phys. Rev. D **99**(11), 115027 (2019). https://doi.org/10.1103/PhysRevD.99.115027
67. U. Ellwanger, C. Hugonie, A.M. Teixeira, The next-to-minimal supersymmetric Standard Model. Phys. Rep. **496**, 1–77 (2010). https://doi.org/10.1016/j.physrep.2010.07.001
68. M. Masip, R. Munoz-Tapia, A. Pomarol, Limits on the mass of the lightest Higgs in supersymmetric models. Phys. Rev. D **57**, R5340 (1998). https://doi.org/10.1103/PhysRevD.57.R5340
69. E. Bagnaschi, M. Goodsell, P. Slavich, Higgs-mass prediction in the NMSSM with heavy BSM particles. Eur. Phys. J. C **82**(10), 853 (2022). https://doi.org/10.1140/epjc/s10052-022-10810-2
70. J. Baglio et al., NMSSMCALC: a program package for the calculation of loop-corrected Higgs boson masses and decay widths in the (complex) NMSSM. Comput. Phys. Commun. **185**(12), 3372–3391 (2014). https://doi.org/10.1016/j.cpc.2014.08.005
71. T.N. Dao et al., Two-loop $mathcalO$ (α_t^2) corrections to the neutral Higgs boson masses in the CP-violating NMSSM. JHEP **08**, 114 (2019). https://doi.org/10.1007/JHEP08(2019)114
72. T.N. Dao et al., Two-loop $\mathcal{O}((\alpha_t+\alpha_\lambda+\alpha_\kappa)^2)$ corrections to the Higgs boson masses in the CP-violating NMSSM. JHEP **09**, 193 (2021). https://doi.org/10.1007/JHEP09(2021)193